Delft University of Technology

LITERATURE STUDY REPORT

AE4020

Optimal Earth-Moon Transfers With A Complete Dynamical Model

Author:
Isabel Ibáñez Jiménez (5483093)

Preface

This literature study entails the beginning of an academic year where research, growth and a new working experience will be the primary objective of my everyday life. It was during a 4-month internship in the DLR's (Deutches Zentrum für Luft- und Raumfahrt) Flight Dynamics team, when I became aware of all the fascinating possibilities that astrodynamics could bring concerning space exploration. Moreover, I became part of a team whose main objective was to use all their knowledge, hard work and eagerness towards every space project that stood in front of them.

I decided that 4 months had not been enough, that I wanted to spend more time learning from the team and working in a project that could be part of a real-life mission one day. Therefore, when I got the opportunity to stay and work on lunar transfers for them, I could not refuse. The Moon, our only natural satellite, the most captivating body when observing it from Earth, and the door to the future of space exploration. What a great way to start a career by learning to optimize the best transfers towards it.

I want to thank my family, who has supported my journey in this amazing path around the world, I want to thank DLR for the trust placed on me, and I want to thank Munich, for making me feel at home. Lastly, I would like to thank TU Delft, who was able to open unthinkable paths for us, who taught me more things in 7 months that I could have ever imagined, and specially, for allowing me to meet the people I admire the most academically and personally, my friends, always part of the Monte Carlo fan club.

Contents

Nomenclature

Symbols and notations

- **C**: Jacobi constant value
- **E:** Earth → $\mathbf{M_E}$: Mass of the Earth
- **G**: Gravitational constant, 6.67 10^{-11} N $kg^{-2}m^2$
- **J**: Jacobi constant function
- $\mathbf{L}_i$: Lagrange point
- **M:** Moon → $\mathbf{M_M}$: Mass of the Moon
- **P:** Spacecraft → $\mathbf{m_P}$: Mass of the spacecraft
- **S:** Sun → $\mathbf{M_S}$: Mass of the Sun
- $\Delta V_{\mathbf{TOT}}$: Total velocity increment
- μ: Standard gravitation parameter, $\mu = G \cdot M$
- μ: In the CR3BP, the mass parameter of the system, $\mu = \frac{m_2}{m_1+m_2}$, with m_2 being the mass of the small primary

Abbreviations

- **LTO:** Lunar Transfer Orbit
- **LLO:** Low Lunar Orbit
- **LEO:** Low Earth Orbit
- **GTO:** Geostationary Transfer Orbit
- **GEO:** Geostationary orbit Orbit
- **WSB:** Weak Stability Boundary
- **CR3BP**: Circular Restricted Three Body Problem
- **J2000**: Earth Centered Inertial frame
- **MJD**: Modified Julian Date
- **ESA**: European Space Agency
- **NASA**: National Aeronautics and Space Administration
- **DLR**: Deutches Zentrum für Luft- und Raumfahrt
- **TLI:** Trans-Lunar Injection
- **LOI:** Lunar Orbit Insertion

Chapter 1

Introduction

The Moon is the Earth's only natural satellite, and its presence has many noticeable and unnoticeable effects on our planet, including to stabilize its wobble on its axis and to moderate its climate, as explained by Rast et al. (2017). This is the reason why it has been an object of study since scientist such as Thomas Harriot finished the first sketch of the Moon's surface with the help of a telescope in 1609, or since Galileo discovered that the Moon had mountains and valleys in that same year, as reported by Chapman (2009). It is therefore not surprising that the Moon was the first target of exploration during the space race. Biesbroek et al. (2000) reports that the Soviet satellite Luna-1 marked the beginning of the lunar exploration, when it flew past the Moon in February 1959, followed by Luna-2, which became the first spacecraft to impact another natural satellite. It was not until Luna-9 (1966) that a spacecraft was able to land softly on the lunar surface, and Luna-16 (1970) was the first robotic sample return mission, able to bring scientifically important samples from areas never visited by Apollo. From the USA side, Apollo-8 became the first manned mission to orbit another world in 1968. In 1969, Apollo-11 became the first manned lunar landing mission.

Even though the last man walked on the Moon in 1972, the scientific interest to return humans to the Moon has been increasing in recent years, becoming a scientific as well as strategic objective for many countries, as it can be used as a testing environment for new technologies, and as a launch platform to planets that are further away than the Earth. This *second Moon race* includes programs such as Artemis, and in particular the Gateway station. From this point of view, many different missions will be required not only concerning the manned module that will take the crew to the Moon, but also missions focusing on the control, communications, refueling and many other objectives which include engineering and scientific satellites. Some of the new scientific objectives, as explained by Russell et al. (2011), are to increase our understanding of the complex interaction of the Moon's surface with its space environment, as single-point measurements from the past are inadequate. In addition, Russell explains that lunar orbits are ideal to observe and study the pristine solar wind or showers of particles that impact the Earth and interact with its magnetosphere, because it spends most of its time upstream of Earth's bow shock. The study of their spatio-temporal ambiguities, three-dimensional characteristics and dynamical evolution is required, as the solar wind buffeting the surface never stays constant.

The economical and technological resources have changed significantly since the first lunar race, increasing the complexity of the missions due to the need of reducing the costs and collecting a greater scientific return using less propellant, hence requiring to make the most out of all new available resources and recent research. All of this links directly to the main objective of this report, which is to conduct a literature study of transfers from Earth to the Moon that lays the theoretical foundation for the creation of a software that is able to optimize these transfers and that can be used by the Deutsches Zentrum für Luft- und Raumfahrt (DLR), where the subsequent study is going to be conducted.

The main focus of this literature study will then be to answer several questions that will lead to the specification of a research question that will be solved throughout the master thesis.

To begin with, the understanding of the transfer environment is required to gain a clear idea of the conditions of the transfer. This environment includes the main gravitational bodies and their orbits, which are the Moon (denoted by M), Earth (denoted by E) and the Sun (denoted by S), and also some other perturbations which may affect the trajectory. This study can be found in Chapter 2.

The next question that needs to be answered is:

What types Earth-Moon transfers are possible? Which ones are the most useful for the current and near-future lunar missions?

To answer this question, firstly, the possible reference frames and problem formulations will be studied in Chapter 3, including the Circular Restricted Three-Body Problem (CR3BP), which is a very useful formulation for the mission design in the Earth-Moon region. One of the most important results obtained in this chapter are the main advantages of each formulation, including when and how they could be used.

Moreover, a general best transfer for all possible initial and final conditions can not be calculated. Therefore, to choose the appropriate transfer strategy, it is very important to understand the possibilities in initial and final conditions, and to decide which ones should be the main focus for the present study. In addition to this, it was also found important to decide in which way these conditions are going to be handled when optimizing the transfers, as this decision can have a big influence on the way the problem is approached. This evaluation is found in Chapter 4.

Once all of the previous aspects have been studied, Chapter 5 conducts an analysis on the main transfer possibilities, their (dis)advantages and the way to calculate them, specially to obtain a first initial guess that can be used for further optimization. Even though many possibilities have been stated, the ones that, for this case including the previous analysis, were found to be the most interesting have been looked at in more detail.

Lastly, to solve this first question completely, the past, current and future possible lunar missions have been analyzed in Chapter 6.

Moreover, a second question is addressed in this report:

Which optimization possibility can achieve the best solution from an engineering perspective? What is the best way to model this optimization? What are the main objectives that should be studied?

To answer this question, a propagator and integrator will be selected in Chapter 7, as an analytical solution can not be obtained. Afterwards, in Chapter 8, an analysis of the different optimization possibilities, the most used ones and their advantages and disadvantages will be conducted. In addition to this, the possible objectives and how to deal with them will also be studied.

Lastly, a brief section including the main verification and validation methods will be included in Chapter 9.

It is important to highlight that this project is going to be conducted with and for DLR, and hence it should consider their requirements and their goals. Their main objective is to generate a software that can become the first step for an operational software able to calculate the maneuvers required for a satellite in an Earth-bounded orbit to transfer to a specific orbit around the Moon in the most optimized way. Operational software require high fidelity dynamical models, and hence the modelling of the environment will be an important aspect to consider throughout this paper and the follow-up master thesis project. Moreover, the software should be robust in two ways: firstly, it must be reliable, meaning that if a feasible solution exists, it should always be found and it must be close to the global optimum. In addition, it will need to be able to deal with the uncertainties that some variables will have

in real missions, including the sensitivity to changes in different parameters and their possible subsequent constraint violations. Furthermore, the software should not depend on additional commercial software, but only on work developed during this thesis and some validated and verified in-house and open-source tools.

Chapter 2

Transfer environment

Throughout this chapter, the transfer environment is going to be analyzed. Firstly, the forces and perturbations that may play a role in an Earth-Moon transfer will be explained. Afterwards, the most important data of the main natural bodies included in the transfer will be given. These bodies are the Moon (M), Earth (E) and the Sun (S). A higher understanding of these bodies, including their orbits, their position in space, and their orientation, will become of prime importance when deciding about the possible approximations for the modelling of the problem.

2.1 Gravitational forces and perturbations

Gravitation is the universal force of attraction acting between all matter. As explained by Faller et al. (2022), it controls the trajectories of bodies in the Solar System and in the Universe, hence including the motion of a satellite from Earth to the Moon. The work from Newton (1687) and Einstein have dominated the development of gravitational theory. Nevertheless, Newton's Law of Universal Gravitation is sufficient even today for all but the most precise applications, as it only excludes Einstein's theory of general relativity, which predicts only minute quantitative differences from the Newtonian theory. Newton's Law of Universal Gravitation states, as found in Britannica (2022c), that any particle of matter (M_1) attracts any other (M_2) with a force (F) varying directly as the product of the masses and inversely as the square of the distance between them (r), acting along the line joining both masses in an attractive manner. Its magnitude is then found in Equation 2.1.

$$F = G\,\frac{M_1\ M_2}{r^2} \tag{2.1}$$

where the gravitational constant, G, has a value of $6.673\ \cdot 10^{-11}\ \mathrm{m^3/(s^2 kg)}$ (Chobotov, 2002). It is important to highlight that this equation refers to the attraction between particles, meaning that if a body is not modelled as a point mass, its distribution of masses is important.

Even though gravitation is the main driver for a trajectory in space, there are additional non-gravitational accelerations which will play a role when modelling an Earth-Moon transfer. Knowing about the main external forces, also called perturbations, and their effects on the trajectory considered, is crucial to decide on which aspects are important to include in the model for the calculations.

Figure 2.1 shows the perturbation sources that have the most important accelerations depending on the altitude of the spacecraft over Earth. Even though this figure focuses in more depth on altitudes closer to Earth, it does give a valuable insight for accelerations even beyond the Moon's distance. Firstly, it can be seen that up to the geostationary orbit's (GEO) altitude, the oblateness of Earth (J_2) has a much larger

effect than the Moon's gravity. This also happens for the drag at low altitudes, but its effect decreases at a much larger rate, reaching a value lower than that of the solar radiation pressure at altitudes higher than 1000 km. The Sun is the third largest body to influence the satellite due to its gravitational field, also larger than the solar radiation pressure for all altitudes. Lastly, it can be noted that the solar radiation pressure has a more or less constant acceleration, its formulation will be found in Section 2.1.1.

Michael et al. (1960) calculates the magnitude of the effects on the Earth-Moon trajectories of the eccentricity of the Moon, the oblateness of the Earth and the solar perturbation. He reaches the conclusion that, for direct transfers, the oblateness of the Earth has the highest impact on the trajectory to the Moon. Even though more analyses have been conducted with better data in the last years, the conclusions reached are the same.

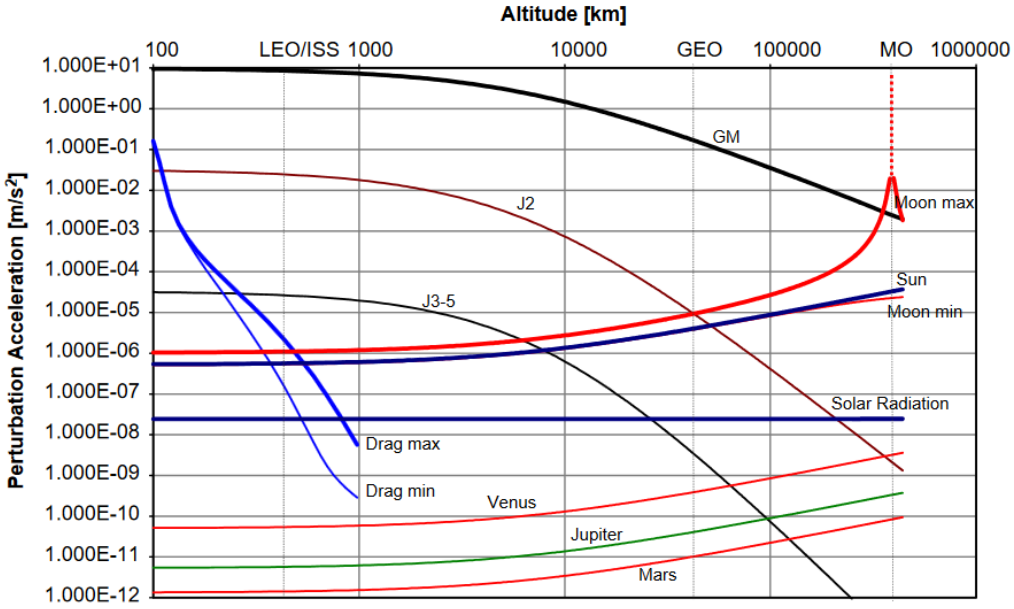

Figure 2.1: Acceleration levels of various perturbation sources for a spacecraft in a geocentric orbit to the Moon. Retrieved from Yazdi et al. (2004).

One of the main objectives of this project, as given in the introduction, is to optimize lunar transfers in a way that can serve as a first step towards an operational software. Therefore, the above-mentioned perturbations will need to be considered, as a minimum, when verifying the final solution.

2.1.1 Solar radiation pressure

The solar radiation pressure is a force produced by the impact of photons from the Sun on the surface of the spacecraft. To calculate its effect on the acceleration, Equation 2.2 is used, as explained by Parker (2018). The satellite reflectivity (C_R) and area (A_{CR}) need to be known, and they depend on the spacecraft. P_{SR} is the solar radiation pressure, taken as $4.560 \cdot 10^{-6}$ N/m^2. The actual mass of the satellite (m_P) changes with each maneuver. $\vec{r_S}$ is the unit vector from the satellite to the Sun. All the calculations assume that the spacecraft's surface is normal to the Sun's direction. In addition, the presence of Earth as an occulting body is to be considered and represented by the factor *illumination*. Figure 2.1 shows that its value is

approximately constant and its effect on the acceleration is of the order of 10^{-7} m/s^2.

$$\vec{a}_{SRP} = -\frac{C_R \cdot A_{CR} \cdot P_{SR}}{m_P} \cdot \vec{r_S}$$
$$\vec{a}_{SRP} = illumination \cdot \vec{a}_{SRP} \tag{2.2}$$

2.2 Moon

The Moon is Earth's only natural satellite, and is the object towards which the transfer is going to be directed. The main data of its orbit around Earth can be found in Table 2.1.

Table 2.1: Main characteristics of the Moon and its orbit. [1] The sideral orbital period is the time that it takes for the Moon to go through 360° around Earth with respect to an Earth Centered Inertial (ECI) reference frame. [2] The synodic period is the period of the lunar phases and is expressed considering the orientation of Earth w.r.t. the Sun. It is larger than the sideral period due to the revolution of Earth around the Sun, which rotates around 30° during one Moon cycle. Obtained from Britannica (2022b).

Parameter	Symbol	Value/units
Perigee	r_p	363104 km
Apogee	r_a	405696 km
Mean semi-major axis	a	384400 km
Eccentricity	e	0.0549
Sideral period [1]	T_{sid}	27.321 days
Synodic period [2]	T_{syn}	29.530 days
Mass	M_M	$7.347 \cdot 10^{22}$ kg
Sphere of influence	R_{sphM}	66,100 km

Moon´s orbit in 3D - Inclination and declination

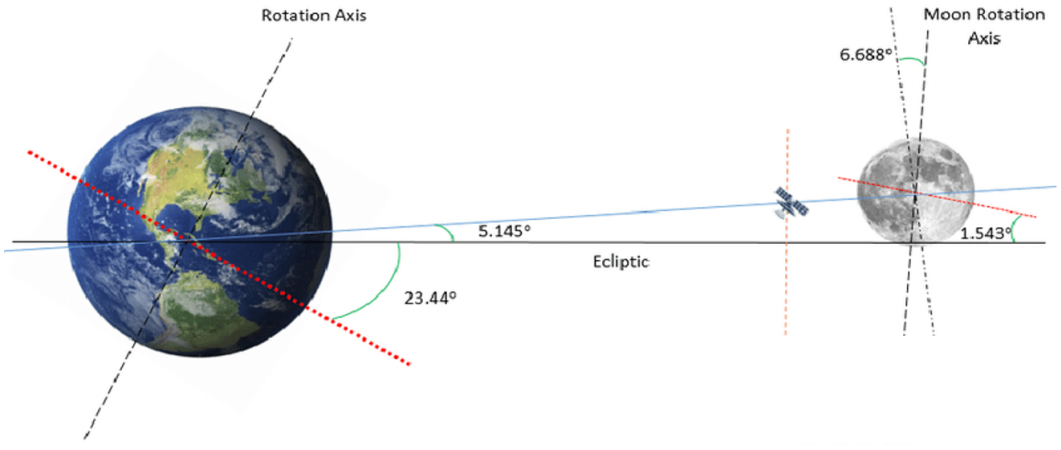

Figure 2.2: Earth-Moon system geometry, not in scale. The red dotted lines correspond to the bodies' equatorial planes. Figure modified from Kara et al. (2015).

The Moon and Earth move in a 3D space. Therefore, to accurately model the motion of the Moon about Earth, an understanding of the angles between the different main planes is required. A sketch of the

Earth-Moon geometry can be found in Figure 2.2. The first important aspect to highlight from this figure is that the Moon orbits Earth near the ecliptic, which is the plane of Earth's orbit around the Sun, with a fixed angle between its own equator and this plane of 1.5424°. This is different to other natural satellites, which tend to orbit their planet near its equatorial plane. The reason why this angle is fixed is because the rotation axis of the Moon is not inertially fixed, and it precesses at the same rate as the Moon's orbital plane, but it is out of phase by 180°.

The mean inclination of the Moon's orbit with respect to the ecliptic is 5.145°. The inclination of the Moon has a period of 173.31 days, and an amplitude of 0.13°. Its greatest value is reached when the line of nodes of the orbit is looking towards the Sun, as explained by Können et al. (1972).

The declination is the Moon's angular distance with respect to Earth´s equator, its value varies cyclically with a period of 27.321 days as the Moon goes around its orbit, with a mean maximum and minimum values of approximately +28.5° and -28.5° respectively. Nevertheless, as explained by Young (2022), its amplitude is not constant and precesses with a period of 18.61 years, while maintaining the tilt relative to the ecliptic. The maximum declination within an orbit can go from 28.585° (23.44° + 5.145°) to 18.295° (23.44° - 5.145°) 9.3 years later. These points are called standstills, and can be found in Figure 2.3. It is interesting to note that they are called standstills because the value of the maximum declination varies only slightly withing three years around these points.

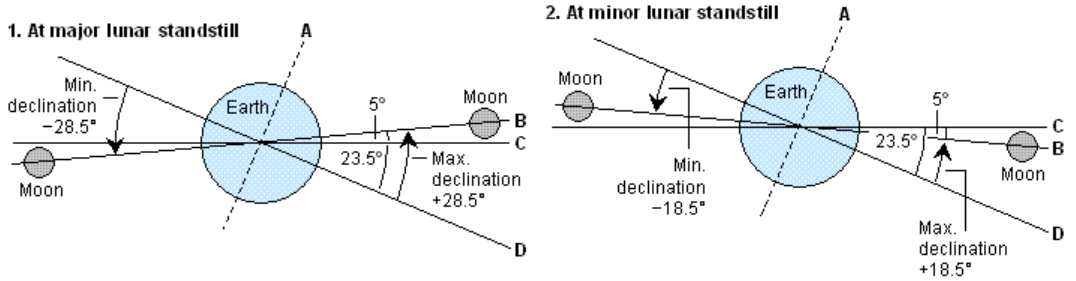

(a) Major lunar standstill.

(b) Minor lunar standstill.

Figure 2.3: Lunar standstills and declination angles. These angles are approximations. A being Earth's rotational axis, B the Moon's orbital plane, C the ecliptic and D Earth's equator. Modified from Wikipedia (2022).

Lastly, the orientation of the Moon´s orbit is not fixed, but also changes with time due to nutation and precession, defined as the variation in time of the rotation axis due to the presence of a near-by gravitational body, visualized in Figure 2.4. Concerning the Moon, one can find the apsidal precession, which changes the direction of the major axes of the ellipse. As explained by Rosengren et al. (2015), it has a period of 8.85 years and moves through a positive rotation about $\hat{h}$, which is the direction of the rotation axis, pointing north. The rotation is then in the same direction as the axial motion of the Moon itself. On the other hand, there is the nodal precession, defined as the time it takes for the ascending node to move 360° relative to the vernal equinox ($\Omega = 0$), it is responsible for the amplitude of the Moon's maximum declination, with a period of 18.61 years.

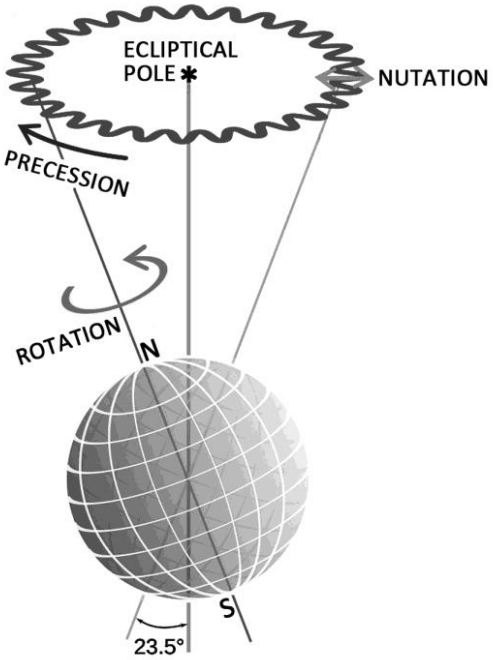

Figure 2.4: Precession and nutation of a body. 23.5° corresponds to the angle between the Earth's rotation axis and the ecliptical pole. Retrieved from Pederzoli (2011).

2.3 Earth

Earth is the main gravitational body for the Earth-Moon trajectories. The main data of its orbit around the Sun can be found in Table 2.2.

Table 2.2: Main characteristics of Earth and its orbit. Obtained from Britannica (2022a).

Parameter	Symbol	Value/units
Pericenter	r_p	$147.10 \cdot 10^6$ km - 0.98329 AU
Apocenter	r_a	$152.10 \cdot 10^6$ km - 1.0167 AU
Mean semi-major axis	a	149,598,262 km - 1.0 AU
Eccentricity	e	0.0167086
Sideral period [1]	T_{sidE}	365.256 days
Rotational period [2]	T_{rotE}	23 hr 56 min 4 sec = 86164 s
Mass	M_E	$5.972 \cdot 10^{24}$ kg
Equatorial radius	R_{eq}	6378.14 km
Mean radius	R_E	6371.01 km
Sphere of influence	R_{sphE}	924,000 km

As seen in Figure 2.2, the rotation axis of Earth is tilted with respect to the ecliptic, and this angle is known as the obliquity. Hohenkerk et al. (1992) explain that the obliquity of Earth suffers from both long- and short-term variations, and its mean value is 23.44°, which remains nearly constant throughout the cycles of axial precession, defined as the slow, and continuous change in the orientation of the body. Earth's cycle lasts approximately 26000 years, hence this value can be taken as constant for the time scale of a mission to the Moon.

One of the most important aspects to consider about Earth is its non-spherical gravitational field, which can have a large effect on the satellite's trajectory if it is close enough to Earth's surface, and whose most important term is typically described by the parameter J_2. As seen in Figure 2.1, the effect on the acceleration that J_2 has on the spacecraft is larger than that of the Moon's point-mass gravity up to around 41000 km from Earth's center.

2.4 Earth-Moon system

The main theory about the way of modelling the Earth-Moon system will be explained in Chapter 3. Nevertheless, in order to bring together all the important data for the problem in one section, the data concerning the Earth-Moon system will be given in Table 2.3. The data includes the position of the Lagrange points and the values for the Jacobi constant related to them. The Lagrange points are equilibrium points found when modeling the system using the Circular Restrictive Three-Body Problem (CR3BP), and the Jacobi constant is a measure of the energy of the system. Both concepts will be explained in more detail in Section 3.2.1.

Table 2.3: Main characteristics of the Earth-Moon system. All the distances are non-dimensionalized with the length units. Data obtained from Belbruno, Gidea, et al. (2010).

Parameter	Symbol	Value/units
Earth-to-Barycenter		4.671 km
Non-dimensional mass	μ	0.0121506682
time unit		$\sim$ 104 sideral month/ 2π
length unit		384400 km
velocity unit		1024 m/s
L_1 x-coordinate	L_1	0.8369147188
L_2 x-coordinate	L_2	1.1556824834
L_3 x-coordinate	L_3	-1.0050626802
Earth/Moon-to-L4/L5	L_4/L_5	1
Jacobi constant for L_1	C_1	$\approx$ 3.2003449098
Jacobi constant for L_2	C_2	$\approx$ 3.1841641431
Jacobi constant for L_3	C_3	$\approx$ 3.0241502628
Jacobi constant for L_4 and L_5	C_4/C_5	$\approx$ 3

2.5 Sun

The third body with highest influence on an Earth-Moon trajectory is the Sun, specially when looking at specific trajectories that make use of its gravity or the instabilities generated in the Earth-Sun system, on the edge of Earth's sphere of influence over the Sun.

Table 2.4: Main characteristics of the Sun. Obtained from USNavalObservatory (2010).

Mass	M_S	$1.989 \cdot 10^{30}$ kg
Mean radius	R_S	696340 km

2.6 Sun-Earth system

The important data concerning the Sun-Earth system will be given in Table 2.5. The non-dimensional position of the two Lagrange points that may play a role in an Earth-Moon transfer, explained in Section 3.2.1, will also be given.

Table 2.5: Main characteristics of the Sun-Earth system. All the distances are non-dmensionalized with the length units. Obtained from Tantardini et al. (2010).

Parameter	Symbol	Value/units
Sun-to-Barycenter		≈ 500 km
Non-dimensional mass	μ	$3.0404234 \cdot 10^{-6}$
length unit		149,598,000 km = 1AU
Earth-to-L1	L_{S1}	≈ 0.0100109943
Earth-to-L2	L_{S2}	≈ 0.0100782578

From this data, and due to the interest for the Earth-Moon transfer of the Sun-Earth L_{S1}, it can be calculated that the distance from the Earth to this point is 1.497623 million kilometers.

Chapter 3

Problem formulations

This chapter will address the different possible problem formulations, specially focusing on the main reference frames that can be used to model a lunar trajectory. In particular, this chapter will study inertial reference frames, specially examining the EME 2000 and its equations of motion, and some rotating reference frames, like the CR3BP including the solutions that using this synodic frame can give, and the planar approximation of it.

At the end of this chapter, a brief explanation on the possible time systems that can be considered during the transfer and in the code will be given.

3.1 Inertial reference frames

An inertial reference frame is defined as that which is not undergoing any acceleration. On the large scale of the Universe, a frame that has its origin on a body and moves with it will never be inertial, as additional external forces will be acting on it. Nevertheless, for the sake of the calculations, and on a smaller scale, these frames are typically considered as "quasi-inertial", explained by Newton (1723).

The most common inertial frame used for Earth-orbiting satellites is the **J2000** (also known as EME 2000) and explained by C. Smith et al. (1989) after it became the main convention established in the International Astronomical Union assembly of 1977. It is an Earth Centered Inertial (ECI) frame with its origin located in the center of mass of Earth. It is defined using Earth's orbital plane and the orientation of its rotation axis, using as a basis Earth's Mean Equator and Equinox at the beginning of year 2000. Its main axes $[X_{J2000}, Y_{J2000}, Z_{J2000}]$ can be defined as follows:

- X_{J2000}: Aligned with the vernal direction at 12:00 on January 1st 2000 .
- Z_{J2000}: Aligned with the Earth rotation axis on that same date.
- Y_{J2000}: Completes the frame using the right-hand rule.

3.1.1 Equations of motion

To express the equations of motion of a satellite it must be noted that all the bodies in the system interact with each other through Newton's law of gravitation. These equations can be written as a summation of gravitational (g) and non-gravitational (ng) accelerations as found in Equation 3.1.

$$\vec{a} = \vec{a}_g + \vec{a}_{ng} \tag{3.1}$$

In general, it is assumed that the mass of the spacecraft is negligible compared to that of the gravitational bodies.

2-body problem

This formulation takes only two bodies into account: the satellite, whose mass is denoted as m_P, and the central gravitational body, with a mass denoted as M_1. The rest non-gravitational accelerations are ignored. It is a useful model because the motion of the spacecraft can be approximated by conic sections, which are predictable and very quick to generate. Therefore, Kepler's equations can be used to relate geometric properties to the orbits that a body follows when it is subject to a central force, as explained in Chobotov (2002). The force acting on the spacecraft is defined in Equation 3.2.

$$\vec{F_g} = m_P \cdot \vec{a_g} \tag{3.2}$$

where the gravitational acceleration ($\vec{a_g}$) exerted by the body of mass M_1 to P is defined in Equation 3.3, having $\vec{r}_{1P}$ as the position vector from 1 to P.

$$\vec{a_g} = -G\ M_1\ \frac{\vec{r}_{1P}}{r_{1P}^3} \tag{3.3}$$

n-body problem

In reality, as found in Figure 2.1, the motion of a spacecraft is actually influenced by multiple gravitational bodies. As defined by Kemble (2006), the equation that can be used to model this n-body problem following the sketch in Figure 3.1 is Equation 3.4.

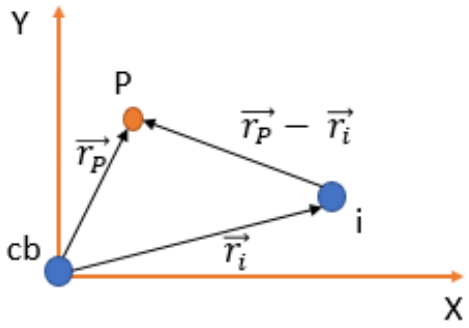

Figure 3.1: Sketch of vectors in the n-body problem.

$$\vec{a}_g = -\mu_{cb}\frac{\vec{r}_P}{r_P^3} + \sum_{i=1}^{n}\left(-\mu_i\left[\frac{\vec{r}_P}{r_P^3} - \frac{\vec{r}_i}{r_i^3}\right]\right) \tag{3.4}$$

where $_{cb}$ denotes the central body and $_i$ the secondary body. $\vec{r}_P$ and $\vec{r}_i$ are the position vectors of the satellite and the secondary body w.r.t the central body body respectively.

It is sometimes complicated to define a dominating body, as it depends on the distance to the third bodies and their perturbations, which can change significantly during the trajectory. The decision is then influenced by the position of the center of the reference frame, as the position vectors of the gravitational bodies w.r.t it are required. For instance, if the center of the reference frame is placed in the barycenter of the system, denoted as B, $\vec{r}_P$ will need to be redefined as $\vec{r}_{BP} - \vec{r}_{Bcb}$, with $\vec{r}_{Bi}$ being the position vector from the barycenter to body i.

Therefore, if multiple gravitational bodies need to be included in the propagation, their positions have to be obtained. This can be done in multiple ways. For instance, in the Solar System, the trajectories of the planets could be propagated following a 2-body approximation with the Sun as the center body, and then use these positions to model the trajectory of the satellite using the n-body approximation. Nevertheless, this is an approximation, as the motion of each planet is also influenced by the gravity field of the rest of the bodies. More accurate models considering these interactions exist, as explained in Section 3.1.2.

3.1.2 Ephemeris model

If a high-fidelity model with high accuracy is needed, the so-called Ephemeris model is required. In it, the motion of a spacecraft under the influence of the gravitational attraction of any or all of the planets and the Moon is approximated using accurate ephemerides that model the motion of these planets relative to the Sun, and are measured in an inertial frame. There are various ephemeris models, however, as explained by Parker and Anderson (2013), the DE421 Planetary and Lunar Ephemerides developed by the Jet Propulsion Laboratory (JPL) and the California Institute of Technology is the most accurate model of the Solar System. In it, the lunar orbit is accurate to within a meter, and the orbits of Earth, Mars, and Venus are accurate to within a kilometer.

In DLR's functions, an ephemeris model is also included based on the equations developed above and Chebyshev coefficients to provide interpolations.

3.2 Rotating Reference frames

These frames co-rotate with the motion of two massive bodies about their barycenter, and are also known by the name of synodic frames. The ones that will be used in this study of an Earth-Moon transfer are the Earth-Moon synodic frame and the Sun-Earth synodic frame. The main model used for planetary transfers is the Circular Restricted Three-Body Problem (CR3BP), whose characteristics will be explained in detail in Section 3.2.1. Nevertheless, other models such as the Planar CR3BP (PCR3BP) and a Four-Body problem can also be used, and will be briefly explained in Sections 3.2.2 and 3.2.3 respectively.

3.2.1 Circular Restricted Three-Body Problem

The CR3BP uses a non-inertial synodic reference frame. A sketch of the model can be found in Figure 3.2.

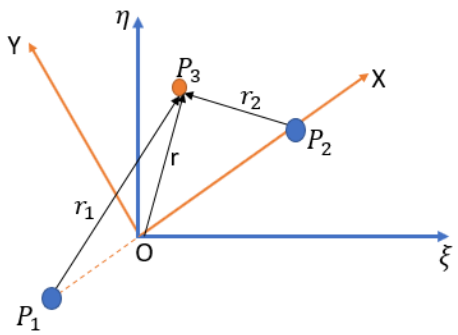

Figure 3.2: Circular Restricted Three-Body Problem (CR3BP) elements and reference frame. The x- and y-components of this rotating coordinate frame can be found in orange. The blue axes are inertially fixed.

This model, as explained in Cowan (2021b), describes the motion of a spacecraft P_3, with mass m_3, under the gravitational influence of two larger bodies, typically called primaries, P_1 with mass m_1, and P_2 with mass m_2. Throughout this paper, P_1 will be designated as primary, and P_2 as secondary. As this problem is not planar, the spacecraft is allowed to move through the entire physical space. The main assumptions of this model are:

- The mass of the satellite m_3 is much smaller than m_2, which is smaller than m_1. This is: $m_3 \ll m_2 < m_1$. The problem is then *restricted*, as the spacecraft does not influence the motion of the primaries.
- P_1 and P_2 move in circular orbits around their barycenter, which is their mutual center of mass. This is the reason why the problem is called *circular*, and the primaries move in their orbits with a constant angular velocity. Hence, P_1 and P_2 move in a single plane, and their motion is held by the conservation of energy and angular momentum, but it is not the case for P_3.
- All bodies' gravitational fields can be modelled as point masses, assuming the bodies are purely spherical.
- The x-axis is defined from P_1 to P_2.
- The z-axis is parallel to the angular momentum direction of the primaries.
- The y-axis is computed using the right-hand rule.

To further define this coordinate system, the magnitudes will be non-dimensionalized with the distance between the primaries. In addition, $m_1 + m_2$ is chosen as the unit of mass, and $1/\omega$ is the unit of time, assuming the angular velocity of the relative motion of the primaries to be one. The equations of motion, as found in Gómez et al. (2001), will then be:

$$\begin{aligned} \ddot{x} - 2\dot{y} &= \Omega_x \\ \ddot{y} + 2\dot{x} &= \Omega_y \\ \ddot{z} &= \Omega_z \end{aligned} \tag{3.5}$$

with the subscripts $_x$, $_y$, $_z$ denoting the partial derivatives of the potential completely defined in Equation 3.6.

$$\Omega(x, y, z) = \frac{1}{2}(x^2 + y^2) + \frac{1-\mu}{r_1} + \frac{\mu}{r_2} + \frac{1}{2}\mu(1-\mu) \tag{3.6}$$

with:

$$\begin{aligned} \vec{r_1} = [\mu + x,\ y,\ z]^T \rightarrow r_1 = \sqrt{(\mu + x)^2 + y^2 + z^2} \\ \vec{r_2} = [\mu + x - 1,\ y,\ z]^T \rightarrow r_2 = \sqrt{(x - 1 + \mu)^2 + y^2 + z^2} \end{aligned} \tag{3.7}$$

This potential accounts for gravitational and centrifugal accelerations but not for the Coriolis term. It produces a non-central force and it is conservative, as it is not time-dependent. Here, $\mu = \frac{m_2}{m_1+m_2}$, and is so-called the mass parameter of the system. It can be noted that as μ approaches zero, the dynamics go towards that of the two-body problem but represented in a rotating frame.

To understand the main characteristics of this problem formulation, it is important to understand the Jacobi constant (C). It is the integral of motion for the system of Equations 3.5, and, as explained by Topputo et al. (2005), represents a 5-dimensional manifold of the problem within the 6-dimensional phase space. It is defined as:

$$J(x, y, z, \dot{x}, \dot{y}, \dot{z}) = C = 2\Omega(x, y, z) - (\dot{x}^2 + \dot{y}^2 + \dot{z}^2) \tag{3.8}$$

To clarify the nomenclature, throughout this work, C will refer to the Jacobi constant value, and J to the function. The velocity included in the definition of the Jacobi constant is expressed with respect to the rotating coordinate system in Figure 3.2, not the inertial velocity. Both the velocity and the position are given in non-dimensional normalized synodic coordinates relative to the barycenter. This constant is a measure of the energy of the system, and as found in Equation 3.8, it is completely defined by the initial conditions, and hence will not change unless the spacecraft is perturbed in some way other than by the gravitational attraction of the two primary bodies. As explained by Mengali et al. (2005), its value gives a Hill region, which is where the spacecraft is energetically permitted to move around. Its boundary is the zero-velocity curve, which varies with the Jacobi energy. These surfaces are symmetric w.r.t. the xz-plane and the xy-plane.

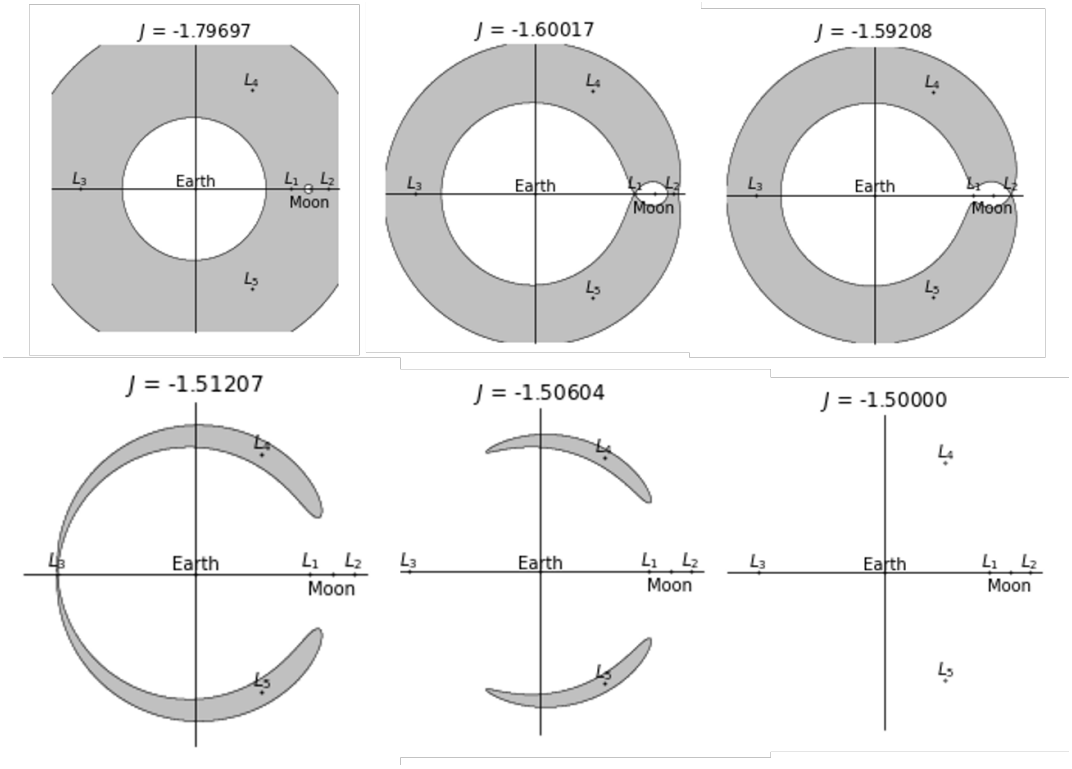

Figure 3.3: x-y representation of Hill spheres in the Earth-Moon system. J is the value of the Jacobi constant. Modified from Weber, 2022.

Large negative values of C describe the motion of the spacecraft bounded to one of the two primaries, as seen in the two left-most upper images in Figure 3.3. Moreover, increasing C would mean that these forbidden regions open at the so-called Lagrange point L_1, hence allowing the spacecraft to leave its primary and reach a region close to the secondary. In addition, as the energy keeps increasing, an approach to the secondary through L_2 becomes possible (upper-right and lower-left images). To reach the region close to L_4 and L_5 requires the highest energy. One can associate a value to the Jacobi constant to each of the Lagrange points, defining them as C_i. Their values for each Lagrange point in the Earth-Moon system can be found in Table 2.3.

In this formulation, the lowest ΔV required to reach the Moon from Earth can then be calculated equating the Jacobi value to C_1. From a generic point ($\vec{r}_0$, $\vec{v}_0$) with constant $C_0 = 2\Omega(\vec{r}_0)$ - v_0^2, and providing a Δv

parallel to the velocity to minimize the constant's variation (with new velocity $v_0' = v_0 + \Delta v$), it can be stated that the new Jacobi constant $C_0' = 2\Omega(\vec{r}_0) - (v_0')^2$ has to be less or equal to $C_1 = 2\Omega(L_1)$. Hence the minimum can be calculated with the only positive root of:

$$\Delta v^2 + 2v_0\Delta v + C_1 - C_0 = 0 \tag{3.9}$$

In addition, another main conclusion to reach for this system are the found symmetries. Miele et al. (2000) showed that if $(x, y, z, \dot{x}, \dot{y}, \dot{z}, t)$ is a solution in the CR3BP, then $(x, -y, z, -\dot{x}, \dot{y}, -\dot{z}, t)$ is also a solution, hence being mirrored in the xz-plane. This is very useful because it shows that there is no need to calculate approach and departure trajectories separately. The other useful symmetry found is that if $(x, y, z, \dot{x}, \dot{y}, \dot{z}, t)$ is a solution in the CR3BP, then $(x, y, -z, \dot{x}, \dot{y}, -\dot{z}, t)$ is also a solution, permitting trajectories to have so-called *Northern* and *Southern* possibilities.

Equilibrium solutions

The equilibrium points, also called Lagrange points or libration points are found where the derivatives of the potential Ω are equal to zero ($\nabla\Omega = 0$). Here, the satellite will not experience any relative acceleration, thus permitting stationary position relative to the reference frame explained before. Their characterization help to understand the flow of the spacecraft in the system. For convenience, the Lagrange points in the Earth-Moon system will be expressed as L_i, and those in the Sun-Earth system as L_{Si}.

The equilibrium points are determined from Equations 3.5, obtaining the constant equilibrium solutions as in McCarthy (2019), and that can be found in the sketch in Figure 3.4.

$$\begin{aligned} x_{eq} &= \frac{(1-\mu)(x_{eq}+\mu)}{||\vec{r_1}||_{eq}^3} + \frac{\mu\ (x_{eq}-(1-\mu))}{||\vec{r_2}||_{eq}^3} \\ y_{eq} &= \frac{(1-\mu)\ y_{eq}}{||\vec{r_1}||_{eq}^3} + \frac{\mu\ y_{eq}}{||\vec{r_2}||_{eq}^3} \\ 0 &= \frac{(1-\mu)\ z_{eq}}{||\vec{r_1}||_{eq}^3} + \frac{\mu\ z_{eq}}{||\vec{r_2}||_{eq}^3} \end{aligned} \tag{3.10}$$

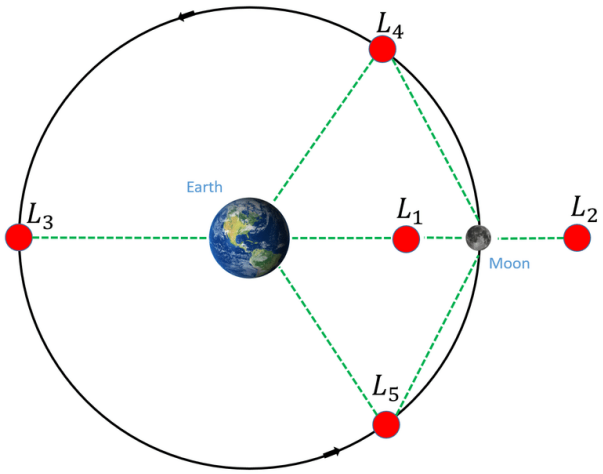

Figure 3.4: Lagrange points in the Earth-Moon system. Retrieved from Gargioni et al. (2019).

Equation 3.10 gives 5 points that satisfy the equilibrium conditions: three collinear points along the x-axis (L_1, L_2, L_3) and the other two (L_4, L_5) being triangular points at the vertices of two equilateral triangles with a common side. All of them can be found in Figure 3.4. From these equations it is easy to note that $z_{eq} = 0$, hence all libration points are inside the x-y plane established in the reference frame found in Figure 3.2.

Stability of Lagrange points

To study the stability of these points, the equations of motion should be linearized by adding a small perturbation around the Lagrange points and then study the subsequent behaviour, as explained by Cacolici et al. (2017). One option is to use Taylor-series expansion. Afterwards, the eigenvalues and the associated eigenvectors are calculated by solving the system. If any of the eigenvalues has a positive real part, that Lagrange point is unstable.

Firstly, it can be stated that all Lagrange points are stable in the z-direction. It is found that the solutions for the xy-plane come in positive/negative pairs for the eigenvalues with real parts, meaning that the system is unstable, hence leaving the purely imaginary eigenvalues as the only stable possibility. For the case of the collinear points, they are found to be unstable saddle points, obtaining one real and one imaginary pair, and hence, defining the dynamics as a saddle times a harmonic oscillator. Nevertheless, as highlighted by Gómez et al. (2001), even if L_1 and L_2 are in a strong unstable equilibrium, the L_3 point has a mild instability, and hence much slower dynamics. For the case of L_4 and L_5, it is found that they are stable if m_1 is significantly larger than m_2 ($\mu \leq 0.03852$), which is the case in the Earth-Moon system and in the Sun-Earth system, giving that the motion around them is bounded.

Invariant manifolds

Looking at the unstable collinear Lagrange point's stability solution, one can find at least one stable and one unstable eigenvalue with corresponding eigenvectors. By perturbing the spacecraft slightly in the unstable direction, the spacecraft will exponentially drift away from the nominal position. In a similar way, with the correct initial conditions, the spacecraft will exponentially approach the point through a trajectory that follows the stable direction. These trajectories are called invariant manifolds, and appear associated to the Lagrange points, which are one-dimensional structures, and to the periodic orbits around them, whose manifolds are two-dimensional structures, as explained by Zazzera et al. (2004).

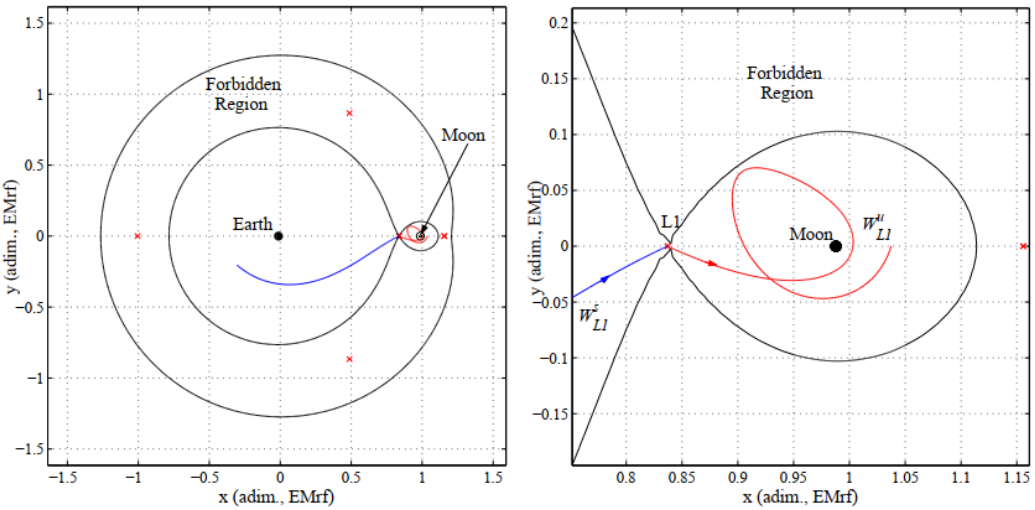

Figure 3.5: The stable (blue) and unstable (red) manifolds associated to the point L_1 in the Earth-Moon system (left). The two are transit trajectories through the small neck opened at L_1 (right). Retrieved from Zazzera et al. (2004).

Figure 3.5 shows a segment of the stable manifold towards Earth and the unstable manifold towards the Moon associated to L_1 in the Earth-Moon system. It has to be highlighted that the stable manifold does not reach a position close to Earth. Even though the propagation is stopped for easier visualization, Zazzera et al. (2004) shows that the minimum distance to Earth seems to be constant and almost equal to 0.35 Earth-Moon unit distances.

Patched three-body model

The CR3BP only considers three-body dynamics. Nevertheless, in many cases, more than three bodies need to be modelled, for instance, when the spacecraft's dynamics are under major influence of the Sun, the Earth and the Moon throughout different parts of its trajectory. One way to overcome this problem, as explained by Parker and Anderson (2013), is to use the patched three-body dynamics, which retains many desirable characteristics of the CR3BP, but allows to include an additional important body. This is done in a similar way as patched-conics in the two-body model, which is by using the Sun–Earth three-body model for all times, except when the spacecraft comes within close proximity to the Moon. Here, the motion is approximated by the Earth–Moon three-body model. The boundary at which to change from one system to the other is called the three-body sphere of influence (3BSOI), and is calculated using Equation 3.11, as defined by Parker (2006).

$$r_{3BSOI} = a \left(\frac{M_M}{M_S} \right)^{2/5} \tag{3.11}$$

Taking the average distance between the Sun and the Moon (a) as approximately equal to 1 AU, and having M_S and M_M as the masses of the Sun and the Moon respectively, the radius of the three-body sphere of influence of the Earth-Moon system is approximately 159,200 km, which includes L_1 and L_2 from this system.

3.2.2 Planar CR3BP

The main difference between the PCR3BP and the generalized one is that, in this case, the spacecraft P_3 is not free to move in the 3D space, but stay in the same plane as the primaries P_1 and P_2. In this case, the initial orbit is assumed to be within this orbital plane, or at least that the ΔV given will include an out-of-plane part that places the spacecraft onto a trajectory in the Earth-Moon plane.

Looking at Tables 2.1 and 2.2, it can be seen that the eccentricity of both the Moon and Earth, and the inclination of the Moon with respect to the ecliptic have low values. Due to this, it has been proven by many researchers, for instance by Koon et al. (2001) or Belbruno (2000), that the planar model can be taken as a good starting point that gives a great insight to the problem, revealing the essence of the transfer dynamics.

3.2.3 Four-Body problem

Some research has also been done to include a fourth body into the model. For instance, in his work, Fernandes et al. (2012) uses the Planar Bicircular restricted Four-Body problem defined by Gomez et al. (2000) to calculate two-impulsive Earth-to-Moon transfers. The fourth body is included starting from the CR3BP and assuming that Earth and the Moon revolve in circular orbits around their center of mass, and that the Earth-Moon barycenter follows a circular orbit around the center of mass of the Sun-Earth-Moon system.

Almeida Junior et al. (2022) was able to conduct a comparison between this model and the CR3BP for a planet-moon system, by taking the term provided by the bi-circular bi-planar four-body problem due to the influence of the Sun as a perturbation, which explicitly shows the difference between both. The main conclusion found is that the difference between models increases mainly due to the masses of the planet-moon system and the distance of the spacecraft from their common barycenter. Even though the Sun–Mars–Phobos system is the system with highest influence of the Sun over the cost of a transfer, the Sun–Earth–Moon will also benefit from the four-body model presented.

3.2.4 Error sources

Some of the main error sources that need to be considered when using these models are:

- The lunar orbit eccentricity is not considered, taking its orbit as circular.
- The Sun's gravitational attraction is not included in the three-body formulations.
- The model for both Earth and the Moon's gravitational field is taken as a point mass.
- Additional perturbations such as the solar radiation pressure and the effect of the gravity of other bodies in the Solar System are neglected.

3.2.5 Rotation-to-inertial coordinate transformation

For a better understanding of these rotating frames, it is important to be able to transform the six-dimensional state (position and velocity) computed in the CR3BP to an inertial frame. This helps to obtain additional insight on the solutions obtained, including the possibility of plotting them in this higher intuitive frame, or, even more importantly, to compute the required ΔV, as it is important to ensure that the rotating components are accounted for. The method includes three steps: the translation of the position and velocity to the first primary, the rotation calculated through a rotation matrix, and the dimensionalization of the magnitudes using the characteristic quantities defined before. This method was explained by Tatay (2019).

Firstly, the translation of the position from the barycenter to an Earth-centered inertial (written as EC) frame with the same x-axis directed towards the Moon is calculated ($\vec{r}_{CR3BP} \rightarrow \vec{r}_{EC}$):

$$\vec{r}_{EC} = \vec{r}_{CR3BP} + \begin{pmatrix} \mu \\ 0 \\ 0 \end{pmatrix} \tag{3.12}$$

For the transformation of the velocity vector, the rotating rate of the system needs to be taken into account. For simplicity, the superscript B will be used to denote the velocity and position of the barycenter (B) with respect to the ECI frame, Ω being the dimensionless rotation rate ($[0\ 0\ 1]^T$).

$$\vec{v}_{EC} = \vec{v}_{CR3BP} + \vec{v}^{B}_{EC} + \Omega \times \vec{r}^{B}_{EC} = \vec{v} + \Omega \times \vec{r}_{EC} = \vec{v}_{CR3BP} + \begin{pmatrix} -y_{EC} \\ x_{EC} \\ 0 \end{pmatrix} \tag{3.13}$$

The position and the velocity are expressed in an Earth-centered inertial reference frame but with its x-axis going towards the Moon. Now, this reference frame needs to be rotated so that it becomes a J2000 inertial

frame. For this rotation step, the rotation matrix is built using the composition of different rotations found in Equation 3.14.

$$R = [R_Z(-\omega - \theta) \times R_X(-i) \times R_Z(-\Omega) \times R_X(-\epsilon)]^T \tag{3.14}$$

where ω, θ, i and Ω are the orbital elements of the Moon, and ϵ is the obliquity of the ecliptic, needed because all the ephemeris are defined with respect to the ecliptic. The velocity and position vectors obtained after the translation will be rotated by multiplying them with the rotation matrix. As a last step, the values should be dimensionalized.

3.3 Comparison between reference frames

Throughout this chapter, a study of different reference frames and problem formulations that are commonly used for the calculations of an Earth-Moon transfer has been conducted, specially focusing on the comparison between modelling the problem in an inertial reference frame or in a rotating reference frame.

Using an inertial reference frame has many advantages. For instance, the equations of motion are well known and can easily incorporate other perturbations into the propagation, such as the solar radiation pressure or the gravity of other bodies whose position can be modelled very precisely using an ephemeris model. Moreover, it can also include the effect that the eccentricity of the orbit of the Moon has on the trajectory. In addition, a 2-body model in an inertial frame gives simple analytical solutions to many aspects of the problem. Moreover, the results can be directly interpreted and plotted, and no extra transformation is required.

Nevertheless, it has a big drawback, which is that some mathematical solutions found in the rotating systems, such as the invariant manifolds, cannot be obtained from an inertial system, hence eliminating the possibility of taking advantage of these useful singularities in the system. In addition, including all the perturbations increases the computational time for each propagation, specially if an ephemeris model is considered. Moreover, these formulations require the Moon to be in the correct position with respect to Earth at the initial time in order to reach its orbit in the final time. These considerations are complicated and will be explained in Chapter 4.

On the other hand, using a rotating frame, and in particular the CR3BP, allows to exploit the dynamics found when analyzing the equations of motion in this new rotating frame, which include the Lagrange points, the invariant manifolds, and the periodic or quasi-periodic orbits. Moreover, in these transfers, the motion of the spacecraft is mainly determined by the two primary bodies, as found in Section 2.1, and the CR3BP is able to include these effects without a large increase in the computations and the computational time of the propagation. In addition, as the reference frame is rotating with the Moon and the time is non-dimensionalized, the initial time is not a determining factor.

However, its main drawback is that it is an approximation that does not allow for an easy modelling of additional perturbations that appear in a real-life situation. Moreover, and even though a useful visualization can be obtained directly from the results in the CR3BP, a transformation requiring a translation and a rotation will be required to reach a final results.

Due to the requirement that the final model must include additional perturbations apart from the point-mass gravity field of the dominant bodies, the last optimization and the results will need to be given in the inertial reference frame. Nevertheless, due to the great advantages that the CR3BP has, the possibility of using the results obtained in this model as the initial guess for a more accurate model where the search space is reduced will be studied. To do so, it has been found that there are open-source and ready-to-use algorithms that model the CR3BP and that can be used to calculate different solutions. One

of these software is SEMPY, a research tool designed by ISAE-SUPAERO for mission analysis in the Sun-Earth-Moon system. It will be analyzed and verified, as it includes several useful features that can be used for this project.

3.4 State representation

The states of the system can be represented in several ways. The most common way is using Cartesian elements, based on a vector of perpendicular distances w.r.t. a reference frame. It is the most used one as it can represent any kind of state. Keplerian elements are highly used when representing two-body orbits in ECI frames, as the full orbit can be modelled knowing the eccentricity, semi-major axis, and inclination. And the position in space of the satellite can be modelled with the true anomaly, which is the angle between the satellite and the perigee, the argument of perigee ω, which is the angle between the ascending node and the perigee, and Ω, which is the right ascension of the ascending node, and represents the angular distance between the vernal equinox and the line of nodes. All found in Figure 4.1. As Keplerian elements are a common way of representing orbits, they will be analyzed when looking at the initial and final conditions. Nevertheless, due to the ease of calculations, the propagations will be conducted using Cartesian elements. Additional state representations are also possible, such as the non-singular elements, but they will not be used in this project.

3.5 Time systems

After having analyzed the main problem formulations related to the different coordinate systems, the most common time systems used for physics and astronomy will also be explained. Time can be defined in countless ways, and a knowledge of the relationship between them is very important for mission analysis. In addition, some of the software functions provided by DLR use different time systems, and hence several transformations may be required. (USNavalObservatory, 2010)

TAI: International Atomic Time, defined in SI seconds. It is the most precise time-keeping and it is based in the combination of 400 atomic clocks. It is determined by the wavelength of radiation of a cesium atom.

TT: Terrestrial Time. Defined to be consistent with SI second (from TAI) and the General theory of relativity. It is mainly used by astronomers to measure the planetary positions in relation to Earth's center.

UTC: Coordinated Universal Time. It is the main time standard that regulates the world's clocks and times, and it is available from radio broadcast signals. Leap seconds are added to compensate for the accumulated difference between TAI and the time measured by Earth´s rotation. These leap seconds are tabulated, and need to be given as inputs in the software.

MJD: Modified Julian Date. Number of days since midnight on November 17^{th} 1858, corresponding to 2400000.5 days after day 0 of the Julian calendar, as explained in WolframResearch (2007). This time conversion is used to facilitate chronological calculations, numbering all days in a consecutive way.

ET. Dynamical time (Ephemeris time). Its duration is based on the orbital motion of Earth, the Moon and planets, as it refers to the independent variable in the equations of motion governing the bodies in the Solar System. It has been used to develop the numerically integrated Solar System ephemerides produced at JPL.

To change from TT to UTC, a table containing the the pole axis coordinates (ERP) is needed. Every time a leap second is added to UTC the separation between UTC and TT grows even more. Currently, TAI

- UTC = 34 leap seconds. The difference between TT and TAI is approximately 32.184 s. And between TAI and ET (ET-TAI) is 32.184 s + relativistic terms, which contribute to less than 2 milliseconds, as found in Parker and Anderson (2013).

For the problem at hand, the main time system that will be used is the MJD, as it allows for easier chronological calculations.

Chapter 4

Initial and final conditions

One very important decision to make when looking to optimize Earth-Moon transfers is to decide which type of initial and final states are going to be given. The possibilities include to give initial and final orbits with the exact position and time, or making it more general by giving a specific orbit from which to depart or where to arrive at. A study of the different possibilities will follow in this chapter, in addition to a characterization of the different possible orbits. Moreover, this decision will also have a big influence on the decision of the best transfer possibility to optimize, as a general best transfer orbit for all possible initial and final orbits cannot be calculated

4.1 Initial state

There are many possibilitiesfor the description of initial states. Firstly, to give an exact position, velocity and time, as will be presented in Section 4.1.1. Secondly, Section 4.1.2 gives a more general option, which would be to give the information of the orbit the satellite is in, but not the exact position and velocity. A third possibility would be to start from the launch site on the surface of Earth, giving the available launch window as initial time. Nevertheless, and even though this possibility will add a higher understanding of the required ΔV for the whole mission, this possibility has been discarded due to the great difficulties that it would bring to conduct an accurate analysis of the launch phase, which is out of the scope of this project. Moreover, accurate information of the reachable orbits for the most common commercial launchers in addition to the ΔV required is available.

Due to the main objectives of this project, the initial states will be constrained to Earth-bounded orbits, and hence no option such as starting from a periodic orbit in the CR3BP will be considered.

4.1.1 Initial position, velocity and time

Here, the initial conditions will be given as:

$$\left[\vec{x}_0,\ \vec{\dot{x}}_0,\ t_0\right]^T = [x_0,\ y_0,\ z_0,\ \dot{x}_0,\ \dot{y}_0,\ \dot{z}_0,\ t_0]^T \tag{4.1}$$

The main advantage of having an initial condition expressed like in Equation 4.1 and not as an initial orbit is that the solution obtained will always be plausible when the satellite is at that position in the exact time. It is straightforward and does not require extra thought on how to get the satellite to the wanted point, as it is given as input.

Nevertheless, one of the main disadvantages is that, if the calculations are conducted beforehand, meaning, for instance, before launch, the exact position and time will not be completely known, and may vary depending on delays in launches. This possibility will therefore make the code very specific and dependent on the launch. In addition, the values will need to be found and/or calculated in a previous step.

Moreover, it is important to take into account that transfers in the CR3BP are very dependent on the initial state, hindering convergence in the optimization process.

4.1.2 Initial orbits

The initial orbits considered are Keplerian orbits, which can be modelled both in the 2-body problem and in the CR3BP. The study will only focus on closed orbits as initial orbits, excluding possible parabolas and hyperbolas. The possibilities studied are LEO, GEO and GTO orbits, explained below. But first, the elements that define a closed orbit around the Earth can be found in Figure 4.1.

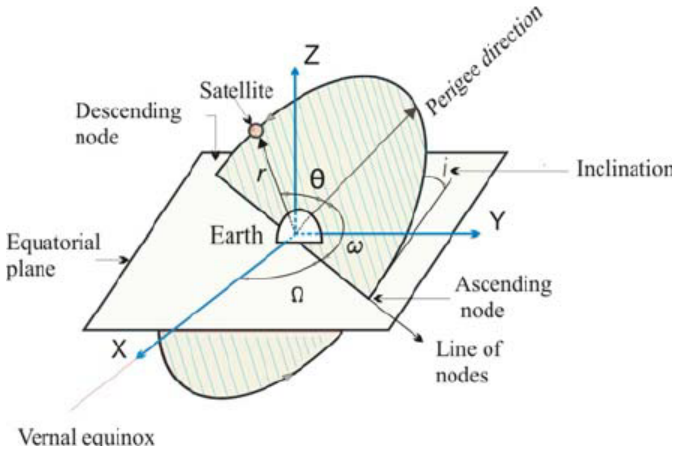

Figure 4.1: Space orbital parameters. Retrieved from Cakaj et al. (2007).

- **Low Earth Orbit (LEO):** LEOs are referred to those orbiting around Earth at an altitude of maximum 1000 km, but can go as low as 160 km. LEOs can have all different inclinations, but their eccentricity cannot be higher than approximately 0.25. Satellites in a LEO will go around Earth more than once a day. For instance, the ISS, which is in a LEO at a mean altitude of around 408 km, will travel at roughly 7.8 km/s, taking around 90 minutes to circle Earth. At this altitude, the effect of the non-spherical harmonics in Earth's gravity field and other perturbations such as the drag do play a noticeable role in the satellite's orbit if it stays in this parking orbit for a long time.

- **Geostationary Earth Orbit (GEO):** The GEO is a specific geosynchronous orbit. Here, the spacecraft will travel at the same speed as the rotation of Earth, meaning that it is at a distance of around 42,164 km from the center of Earth (an altitude of roughly 35,786 km). In addition to that, a geostationary orbit is circular and equatorial.

- **Geostationary Transfer Orbits (GTO):** It is a highly elliptic orbit with a perigee at a LEO altitude and an apogee at the GEO altitude. Many launchers are designed to place the satellites they carry in this GTO. It is important to take into account that many nanosatellites can now be taken as secondary payloads (or as piggyback) in large launchers that take bigger satellites to GEO, making these missions cheaper, and hence making the GTO a very plausible initial orbit. Nevertheless, it is important to consider that in these cases, the launch window cannot be chosen, nor can a neat specification of the initial orbit even if it will bring great advantages for propellant

savings. In addition, the specific position in the objective orbit cannot be known in advance. When looking at the GTO, it can be noticed that it goes through the Van Allen Belt, a region around Earth with energetically charged particles captured by the magnetic field. Long exposure to this radiation can bring problems to both the crew and to sensitive components in the satellite, which need to be shielded.

The parameters required to completely define each of the orbits above are very similar, so all three possibilities can be taken as one in the project.

Time

The way to deal with time is a complicated question when deciding to give an initial orbit as the initial state. This is due to the fact that the geometry of the system and hence the most optimal solution is time dependent, so the actual initial epoch, mostly expressed in MJD, is something to consider. The questions that come up when thinking about this issue are: Where will the spacecraft be at the time of departure? This is given by the true anomaly θ, which goes from 0° to 360°, covering the whole orbit, and which is measured with respect to the location of the pericenter. It is important to consider that the direction to the pericenter might be changing due to the perturbations, and that it might be ill-defined, as is the case for circular orbits. Therefore, another angle expressed the same way as the true anomaly but with respect to a different reference axis can also be used in some cases. Nevertheless, in many applications, the exact value of the initial time or angle are not known, as the optimization is conducted prior to launch. Therefore, and accepting that it will not be a fixed value at which to depart, keeping it as a free variable inside some given limits is an option to consider. Afterwards, the real position can be adjusted through phasing orbits.

For instance, if a satellite is launched as a piggy-back, there will be no control over the launch date and time. One possibility studied by Quantius et al. (2012) to handle this issue is having the launch date completely unknown, while assuming the launch time to be within the standard launch window of the rocket (Ariane 5). Others such as Ceriotti et al. (2006) deal with the problem by considering various launch opportunities, which generate different mission timelines.

Table 4.1: Orbital elements of the standard GTO of Ariane 5. Obtained from *Ariane 5 User's Manual* (2008).

Parameter	Symbol	Value/units
Inclination	i	6° to the equator
Altitude of perigee	Z_p	250 km
Altitude of apogee	Z_a	35943 km
Argument of perigee	ω	178°
Longitude of the ascending node	Ω	Determined by launch epoch

4.1.3 Initial state comparison and decision

As explained before, giving as the initial state the initial position, velocity, and time, will ensure that the solution obtained is the most optimum one for the known case, and will be the beginning of a straightforward approach. Nevertheless, it makes the optimization much less general, and the code may become less useful for the calculations conducted before launch in a mission planning phase.

On the other hand, having as an initial guess an initial orbit with the specified parameters will make the algorithm less tied to the before-hand calculations of the exact trajectory of the spacecraft at that time, hence becoming more general. In addition, it is well known how to translate the specific point in an

orbit to position and velocity vectors. However, this option has the drawback that time becomes an extra variable that needs to be dealt with with care.

Looking at both options, and always considering the main objective of the project, the **initial states will be given as initial orbits**, in a way that all Earth-bounded orbits can be included, not constraining it to circular orbits which would leave out the possibility of a GTO as an initial case. Moreover, this decision also leaves open the possibility of having other orbital parameters as free variables.

4.2 Final state

The final state and how to define it is also required for a good modelling of the problem. For the definition of final state, the only option that makes sense is to give the target orbit and ensure that, after the optimization of the trajectory, all its parameters are reached. The decision to be made in this case is which types of orbits are going to be defined as the objective ones for the problem, therefore, an analysis of the different options, their advantages and disadvantages is conducted in this section.

Two kinds of orbits will be looked at. Firstly, nominal orbits around the Moon, which can be modelled using the nominal 2-body problem. Secondly, periodic and quasi-periodic orbits around the Lagrange points, which cannot be modeled using a 2-body problem, and are a result from the CR3BP formulation.

4.2.1 Keplerian orbits

One of the most interesting places on the Moon's surface from a scientific point of view for the current lunar exploration are the lunar poles. It has been found that deep polar craters may contain ice, which could be harvested and melted by astronauts for drinking, or to split into hydrogen and oxygen for rocket propellant and other uses. Therefore, constant communication to the poles would be required.

Due to the features obtained from the gravitational field of the Moon combined with that of Earth, unique orbits around the Moon that are very useful for lunar exploration can be found. These include **Lunar Frozen orbits (LFO)** which are orbits where the natural drift due to the gravity field has been minimized by careful selection of the orbital parameters, reducing and/or eliminating the need of station-keeping but at the same time maintaining their usefulness for science.

The most stable orbits around Earth are circular and equatorial. Nevertheless, it was found by many researchers including Folta et al. (2006) that this is not the case for lunar orbits. Firstly, they explain that operational experience has shown that lunar orbits at altitudes larger than 750 km have their dynamics dominated by Earth perturbations and hence become very unstable, specially for circular equatorial orbits. Nevertheless, it was found that high-inclination, highly elliptical orbits can become frozen orbits, hence being the cheapest and most stable for communications satellites around the Moon. For instance, for coverage of the south pole, an orbit with an eccentricity of about 0.6 is desired. It can also be highlighted that for gravitational experiments, relatively low orbits are desired, and to cover most part of the Moon, orbits with a high inclination, for instance **polar orbits**, are recommended.

Low Lunar Orbits (LLO): They are orbits with an altitude lower than 120 km and a period of around 2 hour. They are very useful for many scientific reasons, but are, in general, unstable due to the large gravitational perturbation effects. Therefore, if the objective is to reduce the orbital maintenance, the specific low lunar frozen orbits are required. Some of these frozen orbits have been found by Lara et al. (2009), each defined by a specific semi-major axis, eccentricity and inclination, but they tend to be near-circular and with an altitude varying around 100 km.

4.2.2 (Quasi-)periodic orbits around Lagrange points

Apart from classical orbits around a body in space defined by the 2-body problem approximation, Poincaré (1967) proved the existence of periodic orbits when switching from an inertial to a barycentric rotating frame, for instance the CR3BP, explained in Section 3.2.1, claiming that there is an infinite variety of these periodic solutions. These periodic solutions can not only orbit around each of the primaries, but also around the Lagrange points. A collection of the studies of five different authors including analytical methods to approximate periodic motion near Lagrange points can be found in the work by Moulton (1920). It became the starting point for further analyses possible due to the increase of computational capacity.

It was then studied that these orbits are found with the characterization of a whole family of orbits, as isolated periodic orbits do not exist. To identify each orbit inside a family the parameter that is typically used is A_x, referring to the semi-amplitude in the plane of the primaries, and A_z, being the out-of-plane amplitude.

If the transfer objective are these orbits, and as the final point cannot be represented using simple parameters such as in Keplerian orbits, the points of this periodic orbits need to be calculated numerically and then used directly by the transfer algorithm. In the study conducted by Merritt (1996), 4 specific points are used as possible final conditions inside the Halo orbit. Nevertheless, more points can be used in order to find a more optimum path to the orbit, as phasing is typically not important when looking at the final conditions. However, an increase in the number of points to analyze will lead to an increase in the computational time required to reach the solution.

The orbits that are going to be studied are Planar Lyapunov orbits (PLO), Halo orbits, and some information will be given about Near Rectilinear Halo Orbits (NRHO), Lissajous orbits. and Distant Retrograde Orbits (DRO).

Planar Lyapunov orbits

The Lyapunov orbits were named after the Russian mathematician who became in 1989 the pioneer in analyzing non-linear dynamical system by linearizing them around the equilibrium points. PLOs are the simplest periodic orbits in the CR3BP, as they lay completely in the primaries' plane (i.e., have no out-of-plane component). They exist around all three collinear Lagrange points. As given in Parker and Anderson (2013), L_1 and L_2 PLOs have periods in between 2 and 4 weeks and L_3 orbits of 4 weeks.

According to the Poincaré theorem, explained by Canalias et al. (2007), at a given energy level and so at a given value of the Jacobi constant, there is a unique PLO around each Lagrange point (L_1 and L_2), and it makes a unique periodic motion around the L_i for the planar case. An example of these orbits around L_1 can be found in Figure 4.2. It is also interesting to note that, when the Jacobi constant C is that of the Lagrange point L_i (C = C_i), the zero-velocity curves (or energy curves) collapse, leaving no room for any Lyapunov orbit, hence there is a maximum value of C for which PLOs exist. As seen in Figure 4.2, high values of C correspond to very low y-amplitudes. A minimum value of C can also be established, and is taken when the Lindstedt-Poincaré series can no longer give five accurate results when truncated at order 15. Even with these limits of C, the PLO's amplitude varies considerably depending on the energy level.

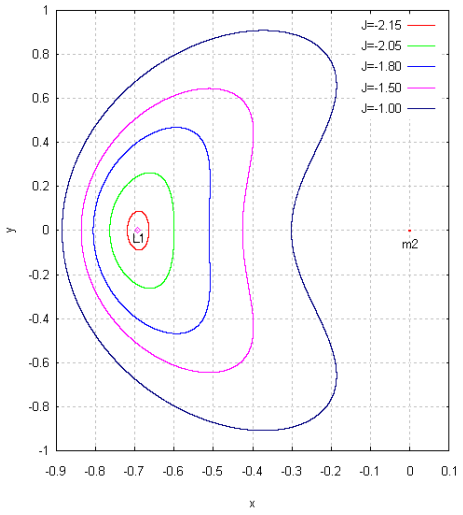

Figure 4.2: Lyapunov orbits around L_1 for different Jacobi constants (J). Retrieved from Nakamiya et al. (2007).

The main way to calculate a PLO is to use a single-shooting strategy, as explained by McCarthy (2019). The procedure starts by defining a reasonable initial state vector ($\vec{x_0}$) that lies on the x-axis, with its only velocity component being along the y-axis:

$$\vec{x_0} = [x_0 \quad 0 \quad 0 \quad 0 \quad \dot{y}_0 \quad 0]^T \tag{4.2}$$

It is noticed that there is no out-of-plane component in the position nor in the velocity, getting a planar solution. The single-shooting strategy is used by constraining the second crossing to the x-axis as perpendicular to this axis. The Mirror Theorem, explained by Roy et al. (1955), ensures that the trajectory will return to the initial position, giving a periodic orbit. An example of the procedure by McCarthy (2019) can be found in Figure 4.3.

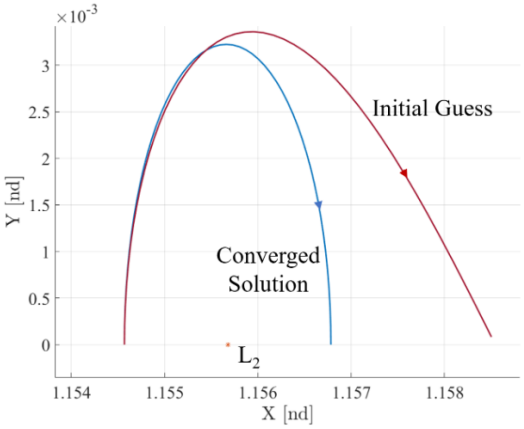

Figure 4.3: Initial guess (red) and final converged solution (blue) for a PLO around the Earth-Moon L_2 using single-shooting strategy with perpendicular crossing. Retrieved from McCarthy (2019).

Halo orbit

The Halo orbits are the most studied orbits in the CR3BP due to their main advantages for operations in the Moon's environment. For instance, a satellite in a Halo orbit around L_2 can provide continuous

communication coverage for most of the Moon's far side, always being visible by this side and Earth. In addition, as explained by Farquhar (1971), if another satellite were placed in L_1, a point-to-point communication network covering the entire lunar surface could also be established.

The main difference between a Halo orbit and a PLO is that it has a component in the plane perpendicular to the plane of the primaries (A_z), which makes them three-dimensional but also causes to exhibit symmetry about the xz-plane. A_z is important as mission constraints can be formulated from its value. For instance, in the same mission as before, a minimum value of A_z is required to ensure non-occultation by the Moon.

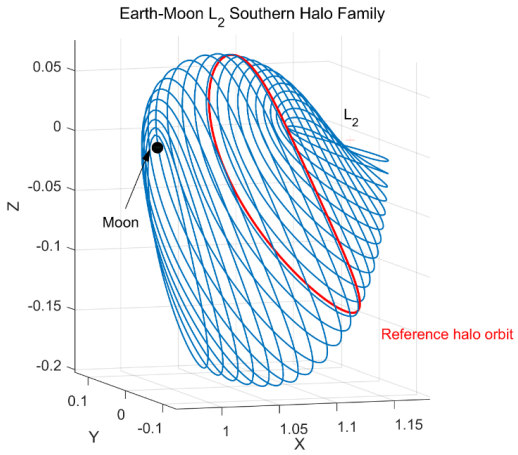

Figure 4.4: Southern Halo family near L_2 in the Earth-Moon system. Retrieved from Jung et al. (2017).

The way in which Halo orbits are constructed is very similar to that of Lyapunov orbits.

NRHO - Near Rectilinear Halo Orbit

The planned orbit for the Gateway station around the Moon is the NRHO. As explained by Zimovan et al. (2017), NRHO's are part of the family of Halo orbits, but with bounded stability indices. They are nearly polar. Their main advantage is that they have favorable stability that allows satellites to maintain their motion with a very low propellant consumption. Zimovan also describes how some NRHO's are very useful to avoid eclipses due to their resonance properties. Another advantage that the NRHO's offer is the feasible transfer options to the lunar surface and other orbits in the cis-lunar space.

Lissajous orbit

They are quasi-periodic trajectories that include components in the plane of both primaries but also perpendicular to it. They follow Lissajous curves, are usually not periodic, and the horizontal and vertical motions do not have the same period, which is the case for Halo orbits, hence imposing less constraints to the mission designer, as explained by Alessi et al. (2010). These orbits can be computed using the Lindstedt-Poincaré method, able to find the semi-analytical series expansions for invariant objects such as orbits and manifolds in terms of suitable amplitudes and phases.

Distant Retrograde Orbit

A DRO is a highly stable orbit around the Moon because of its interactions with L_1 and L_2. It is "distant" because it has a high altitude over the Moon's surface, going above the Lagrange points, and "retrograde" because it follows the direction opposite to that of the Moon around Earth. As explained by Sidorenko (2014), in the synodic (rotating) reference frame, a DRO looks like an ellipse whose center is slowly drifting in the vicinity of the minor primary body. On the other hand, in the inertial reference frame, the third body is orbiting the major primary body. Although being away from the Hill sphere of the minor primary,

the third body permanently stays close enough to it. This orbit will be the one that Orion follows during Artemis I, to collect data and assess the performance of the spacecraft.

Computations using quasi-periodic orbits as final states

The quasi-periodic orbits can not be directly represented in the reference systems without previous computations that give discrete solutions. Therefore, the best way to include these orbits as final states is by discretizing the target orbit in various points in order to make a linear approximation of the problem and be able to solve it through its eigenvalues and relative eigenvectors. Afterwards, the state can be perturbed and backward-propagated in the direction of stable eigenvectors to find the stable manifolds that lead to these orbits. Then, the full connection with the initial state has to be found.

4.2.3 Lunar surface

Another possible final destination is the lunar surface which requires a designed flight path angle. However, this option has been discarded because most of the missions go to a lunar orbit before landing on the surface.

4.2.4 Final state comparison

For the final state, both Keplerian orbits around the Moon and quasi-periodic orbits have been studied.

The main advantage of Keplerian orbits around the Moon is that they can be modelled both in the CR3BP and in an inertial frame, or in a 2-body problem using Keplerian elements. Furthermore, they are simple, they have been used in many missions, and they offer solutions for many scientific and engineering interests such as for communication with the lunar south pole. One of the disadvantages that they have is that they are not static in an inertial reference frame centered on Earth, which may complicate the calculation of the final injection.

On the other hand, periodic and quasi-periodic orbits offer the opportunity to exploit the dynamics of the CR3BP, and many include aspects that can be beneficial for missions and operations to the Moon, which is the reason why they have been greatly studied and chosen as objective orbits in recent years. In addition, they are static in the CR3BP, and hence they do not change with time. Nevertheless, they have a big drawback, which is that they cannot be modelled directly, as is the case for Keplerian orbits. To use them as a final state, they need to be generated beforehand in a discretized manner, and the state for each individual point needs to be calculated and stored. In addition, they require the use of the CR3BP, as they cannot be generated in an inertial frame.

After having analyzed the final states, the main focus of the thesis will be to consider **Keplerian orbits** due to their advantages, and because they can be modelled in an inertial frame. Moreover, including quasi-periodic orbits induces the need of additional computations which may become very time consuming, and are not part of the main requirements of the software. Nevertheless, these orbits do offer great advantages, and hence are an interesting topic for further study.

Chapter 5

Transfer Possibilities

Throughout this chapter, the main transfer possibilities to get from Earth to the Moon will be explained, including their main advantages and disadvantages in order to decide which one best suits the problem at hand. These include direct transfers, bi-elliptic transfers, weak stability boundary transfers, manifold transfers and transfers using fly-bys.

5.1 Direct transfers

Direct transfers are the simplest way of transfers from Earth to the Moon. They are defined as transfers where the dynamics are dominated by the gravitational attraction of Earth and Moon, and where all other forces can be considered as perturbations. They rely on a maneuver typically performed in the perigee of the initial parking orbit around Earth to get the satellite into a Lunar Transfer Orbit (LTO) with an apogee close to the Moon's distance at the current time. The first maneuver is commonly called the Transfer Lunar Injection (TLI) maneuver. Upon arrival, a second maneuver is required to get into a lunar orbit with its predefined velocity.

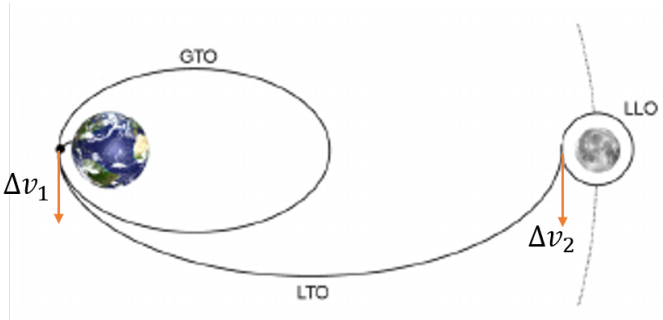

Figure 5.1: Bi-impulsive direct transfer diagram from a GTO to a LLO, including two impulsive maneuvers parallel to the velocity in the perigee and apogee of the LTO. Figure modified from Lange et al. (2008).

The main and simplest way to model these transfers is using a bi-impulsive procedure, as depicted in Figure 5.1 and defined by Hohmann (1925), meaning that no intermediate maneuvers will be conducted. When these impulses are performed in the perigee and apogee respectively, and tangent to the initial and final orbits, the result is the Hohmann transfer, which is the most propellant-efficient direct transfer. For instance, as found in Topputo et al. (2005) from a LEO with an altitude of 167 km to a LLO with an altitude of 100 km, the ΔV required is 3991 m/s and the time of flight is 5 days.

With a bi-impulsive transfer, if one has an initial circular orbit around Earth (LEO) and a final circular orbit around the Moon (LLO), the ΔV_{TOT} required, calculated by adding the ΔV_{LEO} used to leave the LEO and the ΔV_{LLO} used to get into the LLO, is completely defined by the Jacobi constant of the transfer orbit (C_t) (Equation 3.8), and the radius of the initial and final orbits (R_i, R_f), obtained through the terms v_i, C_i and v_f, C_f. Then, after some derivations calculated in detail by Mengali et al. (2005), and simplifying the results by assuming a low-height initial and final orbits, Equation 5.1 is obtained.

$$\begin{aligned}\Delta V_{\text{TOT}} = \Delta V_{\text{LEO}} + \Delta V_{\text{LLO}} &= \left(-v_i + \sqrt{v_i^2 + C_t - C_i}\right) + \left(-v_f + \sqrt{v_f^2 + C_t - C_f}\right) \\ &= -\left(\sqrt{(1-\mu)/R_i} - R_i + \sqrt{\mu/R_f}\right) + \sqrt{R_i^2 + \mu^2 + 2(1-\mu)/R_i + 2\mu/(1-R_i) - 2R_i\mu + C_t} \\ &+ \sqrt{(1-\mu)^2 + R_f^2 + (2\mu/R_f) + 2(1-\mu)/(1-R_f) - 2(1-\mu)R_f + C_t}\end{aligned} \tag{5.1}$$

knowing that:

$$\begin{aligned} v_i &\cong \sqrt{(1-\mu)/R_i} - R_i \\ v_f &\cong \sqrt{\mu/R_f} \end{aligned} \tag{5.2}$$

and:

$$\begin{aligned} v_i^2 - C_i &= (x_i^2 + y_i^2) + 2[(1-\mu)/R_i + \mu/\rho_{Mi}] \\ v_f^2 - C_f &= (x_f^2 + y_f^2) + 2[(1-\mu)/\rho_{Ef} + \mu/R_f] \end{aligned} \tag{5.3}$$

with μ being the mass parameter of the Earth-Moon system, and ρ_{Mi} and ρ_{Ef} the distance of the satellite from the Moon at the beginning of the transfer and from Earth at the end of the transfer respectively.

These calculations an be performed because C_t is a measure of the energy of the system in the CR3BP, explained in Section 3.2.1. Even though this derivation is done using the planar CR3BP, and assuming tangential burns and low heights of the initial and final orbits compared with the Earth-Moon distance, many useful conclusions can be reached. Firstly, ΔV_{tot} increases with C_t. Moreover, that the minimum ΔV_{tot} can be easily found, and is obtained when $C_t = C_{L_1}$. However, this value is not practical because the transfer time becomes infinity when C_t approaches C_{L_1}. This is the reason why it is important to include a maximum allowable transfer time when looking at direct transfers.

Nevertheless, there are several more possibilities. A **mid-course maneuver** may be included to obtain the required inclination with a lower ΔV, following the same principle as that of bi-elliptic maneuvers. It should be done just before getting to the sphere of influence of the Moon, to reduce the required propellant consumption. This maneuver is only possible if there is a small declination angle at the time of encounter, as explained by Seefelder (2000), hence this declination is the main parameter which determines the feasibility of this strategy.

Another possibility for a Hohmann transfer with plane change, as explained by Chobotov (2002), is to **divide the out-of-plane maneuver** (split plane-change of Δi) in between both maneuvers of the bi-impulsive procedure. At the same time as the first ΔV, the satellite will get into the transfer orbit and perform a plane change of α_1, within the second ΔV, the orbit will be circularized and the orbital plane will be further rotated over an angle $\alpha_2 = \Delta i - \alpha_1$.

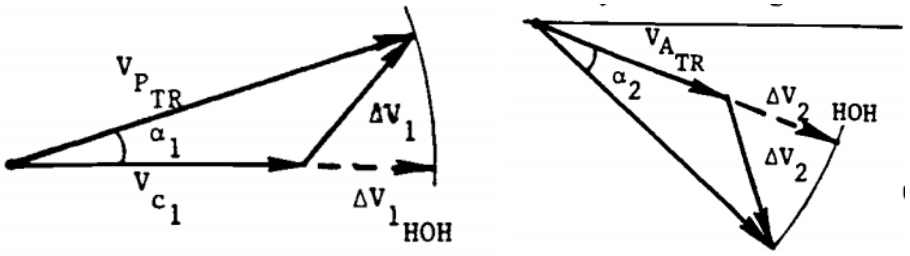

(a) First maneuver.

(b) Second maneuver.

Figure 5.2: Split plane-change maneuver. Δv_{HOH} is the velocity increment if it were in the planar Hohmann case, V_c is the circular velocity. α is the inclination change in each maneuver. Figures retrieved from Chobotov (2002).

There is another possibility within the direct transfers where the increment of apogee is done in **many small impulses**, to reduce the gravity losses. Nevertheless, this procedure reduces the advantage of direct transfers, which is the short transfer time. This type of transfers is typically used for satellites with electric propulsion.

5.1.1 Calculation of direct transfers

One important aspect to consider when calculating direct transfers, as explained by Mengali et al. (2005), is that it is important to give a maximum allowable transfer time, specially when admitting flybys. One of the main reasons, as explained before, is that the minimum ΔV_{tot} is reached for an infinite transfer time, hence the short transfer times will not be an advantage anymore.

Miele et al. (2000) conducts an interesting study for Earth-Moon and Moon-Earth transfers. It is found that there are two groups of optimal trajectories, those with clockwise arrival in LLO, and those with counterclockwise arrival. **Both options will be considered for the optimization in this project**. The main conclusions are the following: Firstly, the velocity required to go from the initial orbit to the transfer orbit is nearly independent of the orbital altitude over the Moon's orbit. The braking velocity impulse decreases as the final altitude over the Moon increases. In terms of characteristic velocity and transfer time, counter-clockwise arrival gives slightly better results than clockwise. The performance index used for the optimization by Miele is:

$$\min J = \Delta V = \Delta V_{LEO} + \Delta V_{LLO} \tag{5.4}$$

The equations used for the acceleration of the spacecraft considering both Earth and the Moon's point masses, using an inertial reference frame contained in the Moon orbital plane, centered at Earth, with its x-axis pointing towards the Moon's initial position and the y-axis directed towards the Moon's initial inertial velocity are:

$$\begin{aligned} \dot{v}_{x,p} &= -\left(\frac{\mu_E}{r_{PE}^3}\right) x_p - \left(\frac{\mu_M}{r_{PM}^3}\right)(x_p - x_M) \\ \dot{v}_{y,p} &= -\left(\frac{\mu_E}{r_{PE}^3}\right) y_p - \left(\frac{\mu_M}{r_{PM}^3}\right)(y_p - y_M) \end{aligned} \tag{5.5}$$

Direct transfers can be constructed with a duration as short as hours or as long as a few weeks, nevertheless, it is found that the most propellant-efficient transfers are typically of about 4.5 days.

5.1.2 Lambert's Approach

As followed by Chobotov (2002), Lambert's problem is a two-body analytical method to calculate transfer orbits between two given position vectors in a specified transfer time. It allows for out-of-plane transfers and a variation of the time of flight. It has been subject of extensive research and is greatly used to obtain first approximations for more complex models. According to Lambert's theorem, the transfer time Δt to go from P_1 to P_2 is only dependent on the sum of the magnitude of the position vectors $(r_1 + r_2)$, the semi-major axis (a), and the length of the chord joining P_1 and P_2 (c). Therefore, it is independent of the orbit's eccentricity. Figure 5.3 shows the main parameters of a Lambert transfer between two points.

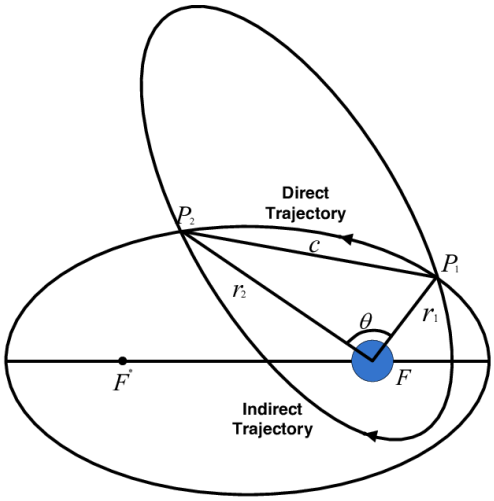

Figure 5.3: Transfer orbit geometry for Lambert's problem. Retrieved from Hosseini (2011).

Knowing that:

$$\begin{aligned} c &= ||\vec{r_2} - \vec{r_1}|| = \sqrt{r_1^2 + r_2^2 - 2r_1 r_2 \cos(\theta)} \\ s &= \frac{c + r_1 + r_2}{2} \end{aligned} \tag{5.6}$$

with c being the chord length and s the semi-perimeter. It can be obtained that the time of flight (Δt) is:

$$\Delta t = \sqrt{\frac{a^3}{\mu}} \left(\alpha - \beta - (\sin \alpha - \sin \beta)\right) \tag{5.7}$$

where:

$$\begin{aligned} \sin\left(\frac{\alpha}{2}\right) &= \sqrt{\frac{s}{2a}} \\ \sin\left(\frac{\beta}{2}\right) &= \sqrt{\frac{s-c}{2a}} \end{aligned} \tag{5.8}$$

One very interesting conclusion to reach from the analysis of these equations is that there exists a minimum semi-major axis length $a_{min} = (r_1 + r_2 + c)/4$ for which it is possible to have both points in the same orbit. To ensure that a solution exists, the minimum time of flight corresponding to a parabolic case can be calculated as well as the maximum time of flight related to a_{min}. To solve Lambert's equation, several

options can be used including Newton iteration, series expansion or a bisection method. The quickest method, as explained by De La Torre et al. (2018) and the one that will be chosen is to use a first-order Taylor's expansion as:

$$\vec{x}^{i+1} = \vec{x}^{i} - DF(\vec{x}^{i})^{-1} F(\vec{x}^{i}) \tag{5.9}$$

with $DF(\vec{x})$ as the Jacobian matrix, which is the matrix containing all first-order partial derivatives of a vector-valued function (F).

As can be seen, Lambert's problem has an analytical solution in the 2-body problem. Nevertheless, in the CR3BP, an iterative procedure is required, becoming a time-fixed single-shooting problem with thirteen variables. Four fixed variables (x_0, y_0, z_0, Δt), three free variables ($\dot{x}_f$, $\dot{y}_f$, $\dot{z}_f$), three constraints (x_f, y_f, z_f) and three unknowns ($\dot{x}_0$, $\dot{y}_0$, $\dot{z}_0$). Here, $_0$ refers to the initial point and $_f$ to the final point.

5.1.3 Patched conics

The patched conics approach relies on a Keplerian decomposition of the Solar System dynamics. Therefore, the spacecraft is assumed to move in a classical 2-body problem, being dominated by the gravity of Earth until reaching the Moon's sphere of influence. From then on, the spacecraft will only be influenced by the Moon's gravity field. Therefore, in direct transfers, the gravity of the Sun will never be considered, as the satellite will always be inside the sphere of influence either of Earth or of the Moon.

The radius of the sphere of influence of a body is calculated as:

$$r_H = a_p \left(\frac{m_{small}}{3 \cdot m_{big}} \right)^{1/3} \tag{5.10}$$

a_p is semi-major axis of the orbit of the body with smallest mass, m_{small} and m_{big} are the mass of the small body and of the large body respectively. Using the data from Chapter 2, one can find that the radius of the sphere of influence of the Moon w.r.t. Earth is of around 60,000 km, and of Earth w.r.t. the Sun is of around 1.5 million km. It is important to note that this equation is different than that of the sphere of influence used for two patched CR3BP, found in Section 3.2.1.

Figure 5.4 shows a sketch of the patched conics procedure. As can be seen and explained by Chobotov (2002), the change of the reference frame when entering the lunar sphere of influence results in a selenocentric (lunar) hyperbola since the velocity of the satellite inside this sphere is finite with respect to the Moon.

There are many ways to model and make use of the patched conics procedure, always considering the required continuity between both conics. One possibility, as explained by Mengali et al. (2005), is to force the trajectory to go through a particular point, which should be on the border of the Moon's sphere of influence, and it should have its abscissa coinciding with that of the Lagrange point L_1. Then, forward and backward propagation should be conducted respectively to find the required ΔV.

This method relies on several approximations. For instance, as explained by Zazzera et al. (2004), the concept of sphere of influence requires the trajectory to rapidly cross the regions at the boundary of the spheres in order to assure a good level of approximation. Hence, the spacecraft should have high relative velocities, which leads to high energy levels.

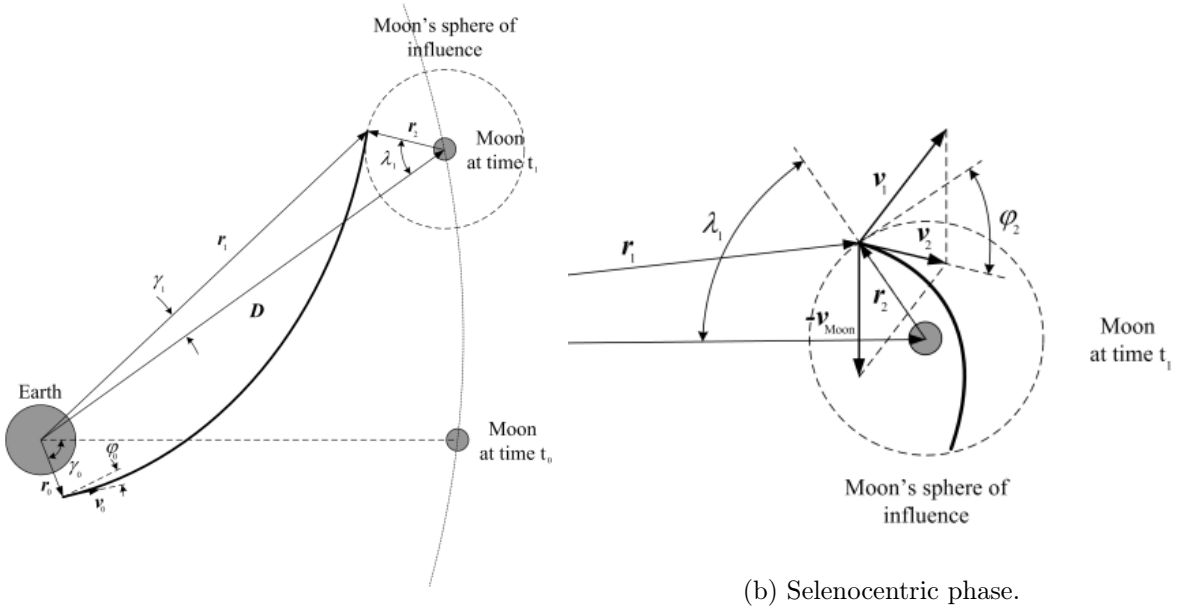

(a) Geocentric phase.

(b) Selenocentric phase.

Figure 5.4: Patched conic approximation. Retrieved from Fernandes et al. (2012).

5.1.4 Orbital Timing

The orbital timing is crucial to model a trajectory that includes more than one gravitational body, as their position in space and time are directly linked with the outcome of the transfer. Orbital timing is something to consider for every transfer possibility, even if for some transfers it is more critical than for others, hence the explanations provided in this section can be taken for other types of transfers.

For a direct transfer, the main reason to consider the orbital timing is to allow the Moon to move into the correct phasing angle to make the transfer. In theory, direct transfers could be conducted twice a day if the inclination of the launch site (or that of the orbit) is larger than the declination of the Moon at that time, or twice a month (minimum number of times), where the Moon is in its ascending or descending node with respect to the equatorial plane. Hence, for circular and equatorial orbits, the lunar transfer windows will open, on average, every 13.6 days. If a direct lunar transfer is followed from a GTO, usually the Moon can only be reached without a plane change if the line of nodes of the GTO and those of the Moon orbit coincide. In addition, as explained by Quantius et al. (2012), if the waiting time required is too short, for instance 3 days, it is sometimes advantageous to extend the waiting time until the next opportunity to properly calibrate the thrusters.

To calculate the correct orbital timing, Yazdi et al. (2004) introduced the concept of **transfer window periods (TWPs)**, which are defined as time period between two successive events when departure is possible with a TLI maneuver tangential to the current orbital plane. If this were not the case, an extra ΔV would be needed to change the inclination as to match the orbital declination of the Moon at arrival, and transfers would not be optimum. Nevertheless, Yazdi et al. (2004) found that $\Delta\Omega$ is not constant, but varies with its drift ($\dot{\Omega}$) due to the different perturbations. $\dot{\Omega}$ is a function of inclination (i) and Earth distance. He found that the real TWP length is of about:

$$\frac{180}{n_{Moon} - \dot{\Omega}} \tag{5.11}$$

with n_{Moon} being the mean motion of the Moon which is around 13.2°/day. Yazdi et al. (2004) concludes that the shortest TWPs are related with low inclined, low altitude and low eccentric orbits.

To wait for the correct orbital timing, **phasing orbits** are typically used. Phasing orbits are orbits with increasing apogee where the satellite will stay until the final burn (ΔV_{TLI}) that gets it into the LTO. To increase the apogee, a small ΔV is required and is typically performed at perigee, hence reducing the final ΔV_{TLI}. As explained by Spurmann (2010), phasing orbits add additional benefits to the transfer apart from reaching the desired place in space and time, but also, as the final ΔV_{TLI} is reduced, the effect of maneuver uncertainties are reduced, and so are the gravity losses. This maneuvering uncertainty depends on the period of the last phasing orbit. Moreover, they can be used in favor of the mission by extending the launch periods or compensating for varying launch dates, by reducing the operational risk of the mission, as the time between maneuvers is increased, or even to be able to accomplish the mission when the launch vehicle is not powerful or accurate enough, which was the case for Chandrayaan-1, found in Goswami et al. (2009). A last advantage compared to staying in the initial parking orbit, typically a GTO, is that the Van-Allen-Belt passages are reduced and the disadvantage of a drifting GTO is not present anymore.

Nevertheless, they also have some drawbacks, including an extended duration of the mission, which increases the general costs, and the that orbit goes through the Van-Allen-Belt. In addition, it is important to consider in the calculations that there can be interactions between the phasing orbit apogee and the Moon, which is not desired.

5.1.5 Free-return transfers

Free-return trajectories were designed in the Apollo program in order to ensure the possibility to safely return to Earth in case of mission failure. A more in-depth study of these transfers is given in Section 6.1.

It has been decided that, as the main focus of the missions for this specific software is not going to be manned flight, but rather smaller missions which would require DLR's flight dynamics tools, this requirement will not be included.

5.1.6 CR3BP

As explained by Merritt (1996), calculating direct transfers using the CR3BP is much more complicated than doing so in the two-body problem, as a closed-formed solution does not exist. Therefore, numerical integration is required to propagate the transfer. The equations of motion used can be found in Equation 3.5.

The main approach to calculate these transfers in the CR3BP is to use a single-shooting method, which requires an intelligent initial guess. To obtain it, Lambert's theorem (Section 5.1.2) or the other 2-body approaches can be used. When applying this solution into the CR3BP, the trajectory is likely to fail, as Lambert's problem does not take the Moon's gravity into account. To solve this problem, differential corrections are used. They are based on the difference between the obtained final state and the target one to estimate the required adjustment in the initial state vector, using the state transition matrix. This approach will give a system of 42 differential equations, but it can be greatly simplified to reach a system of 24 first-order differential equations by forcing the initial position components to remain constant and ignoring the final velocity error. The correction is based on linearized equations of motions, which means that the adjustment found is approximate. Nevertheless, after some iterations, it will converge if the error in the initial guess is not very high.

In addition, and due to the chaotic characteristics in the CR3BP which make the final position highly sensitive to the initial state, a single-shooting strategy may have difficulties converging, especially close to

the primaries. This is due to the fact that round-off errors can become too large, and may create large-scale deviations in the spacecraft's trajectory, as explained by Parker and Anderson (2013). Therefore, another option is to use a multiple-shooting strategy. It is based on the discretization of the trajectory in n patched points so that the propagation is done over shorter periods of time, giving better results when using the linearization approximation. Here, the states are adjusted simultaneously. A sketch of the method can be found in Figure 5.5. One of the constraints that should be added, especially for bi-impulsive direct transfers, is the continuity constraint in the intersection of the different segments. The free vector $\vec{x}$ from Equation 5.9 will now have the components of each intersection point, hence obtaining a length of $(6n-3)\times 1$, only leaving the initial position as fixed. Parker and Anderson (2013) also states that these segments can be patched together with very small maneuvers, smaller than those required for station-keeping, to counteract the round-off error built-up in each segment. Nevertheless, as they are small, they will not be included as deterministic maneuvers for the mission.

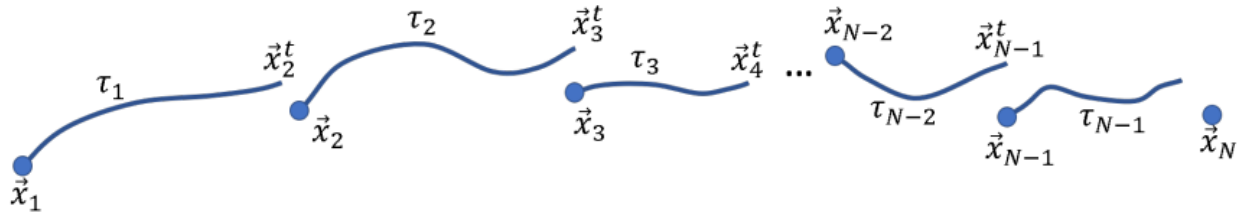

Figure 5.5: Trajectory arcs in multiple shooting scheme. Retrieved from McCarthy (2019).

5.2 Bi-elliptic transfers

The nominal bi-elliptic transfer is a three-impulse transfer between two coplanar circular orbits, as depicted in Figure 5.6. In general, the second impulse (conducted at r_2) can be either in between both orbits or at a radius larger than the higher altitude orbit r_f. This transfer orbit, completely defined in Chobotov (2002), will require a minimum ΔV_{TOT} when $r_2 \to \infty$. With this value of r_2, the orbit will be more efficient than a Hohmann transfer when $r_f/r_1 \leq 11.94$. In addition, the threshold value of r_f/r_1 for which a bi-elliptic transfer will always be more efficient than a Hohmann transfer considering that $r_2/r_1 > r_f/r_1$ is $r_f/r_1 = 15.58$. It is also interesting to note that, for a planar transfer, the maximum savings with, for example, $r_f/r_1 = 50$, is of around 8%, thus reaching the conclusion that a bi-elliptic transfer does not give significant advantages in terms of ΔV_{TOT} compared to a Hohmann transfer, but it does considerably increase the time of flight. Nevertheless, lunar transfers are, in general, not planar, and hence a plane change is required. It is in this situation where bi-elliptic transfers can be very useful.

The changes in the inclination (Δi) of an orbit are the most costly ones, and the ΔV required is calculated using Equation 5.12 (Chobotov, 2002).

$$\Delta V_i = 2\ V_A\ \sin(\Delta i/2) \tag{5.12}$$

with ΔV_i being the required velocity to conduct the maneuver and V_A the velocity at that point. This equation shows that, to reduce ΔV_i, V_A should be reduced as much as possible. Therefore, a useful bi-elliptic transfer, which, as explained by Seefelder (2000), can be used for lunar transfer orbits, consists of injecting the spacecraft into a highly eccentric LTO that has an apogee at around 1 million km from Earth's center (still inside the sphere of influence of the planet), and then conduct a maneuver there to get the spacecraft into a second transfer orbit that reaches the Moon with the correct inclination. To enter the final orbit, a third maneuver is required. It has been proven in Chobotov (2002) that, with large

values of r_2/r_1, a small Δi will mean a large ΔV_{TOT} compared to a direct transfer, whereas for large values of Δi, ΔV_{TOT} is reduced, meaning that the amount of required inclination change is also a factor to be considered when looking at a bi-elliptic transfer over a direct transfer with a plane-change. A thorough investigation has been conducted in Chobotov (2002), and it was found that, for a pure plane-change maneuver (with no change in the orbit's semi-major axis), from $0° \leq \Delta i \leq 38.94°$, the most optimum is to have an $r_2/r_1 = 1$. From $38.94° \leq \Delta i \leq 60°$ it is $r_2/r_1 = \sin(\Delta i/2)/(1 - 2\sin(\Delta i/2))$. And for $60° \leq \Delta i \leq 180°$ it is $r_2/r_1 \to \infty$.

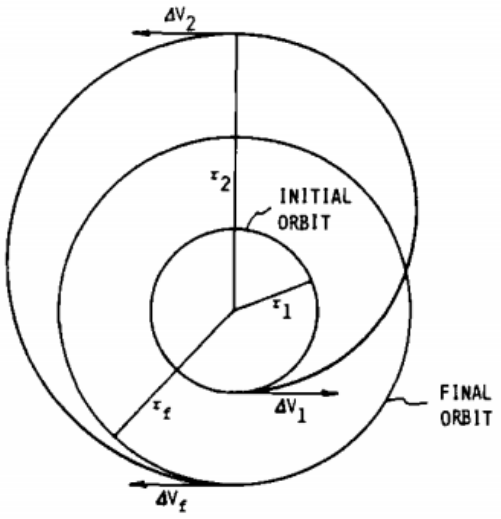

Figure 5.6: Geometry of a bi-elliptic transfer. Retrieved from Chobotov (2002).

5.3 Weak Stability Boundary transfers

Weak Stability Boundary (WSB) transfers have been studied as one of the most promising low-energy transfers from Earth to the Moon, specially since 1991, when the Japanese spacecraft Hiten required an alternative trajectory to reach the Moon and to become captured, as it did not have enough propellant to do so in a conventional direct manner, explained by Belbruno and Miller (1993). These regions and their transfer advantages have been studied by many researchers, especially Edward Belbruno, whose work will be greatly highlighted throughout this section.

5.3.1 Theory and general understanding

The WSBs are regions in the phase space, which is the six-dimensional position-velocity phase space, where the effects of the perturbations due to the Earth-Moon-Sun gravity acting on the spacecraft balance, becoming a transition region between gravitational capture and escape. This yields to very similar accelerations from all bodies, hence resulting in very nonlinear and chaotic dynamics where the spacecraft can be pulled away from the central body by the other bodies' perturbations. The existence of these regions was numerically demonstrated by Belbruno (1987), and it was used to develop the ballistic lunar transfer concept, later used for the Hiten mission, found in Belbruno and Miller (1990). As explained by Belbruno and Miller (1993), the WSB can be viewed as *'a more general and precise estimation of the motion of the sphere of influence'*, and as *'a continuous 3D region about the central mass with the velocity associated to each point of the region depending on the direction of motion'*. It is located around the Lagrange points and it is where both escape and capture from the central body can occur temporarily.

In addition, Belbruno and Carrico (2000) found and verified that this region is a complicated region consisting of many intersections of invariant manifolds, and hence, under some conditions, the points on the stable manifolds are WSB points. An analytical way to calculate this region is also well explained by Belbruno (2000).

5.3.2 WSB transfers

The WSB transfers, sketched in Figure 5.7, also commonly known as low-energy transfers, make use of the characteristics of the WSB region between the Sun-Earth system and the Earth-Moon system. This region gives the satellite the possibility to use the strong solar perturbations to increase the perigee of the orbit to the Moon's distance. In the Earth-Sun system, this region is placed around 1.5 million km from Earth's center (size of the sphere of influence of Earth, and distance where L_{S1} is placed at).

One important aspect to recognize is that, for the transfer to be feasible, the invariant manifold structures need to intersect within each other in a reasonable time, this depends on the configuration of all the bodies, which becomes the prime driver for the success of the approach.

The transfers consist on the following phases:

1. The satellite leaves the parking orbit or the last phasing orbit around Earth in a highly eccentric transfer trajectory towards the WSB region by means of a Trans Lunar Injection maneuver (TLI). This first arc can take around 36 to 45 days. To reach this region using less propellant, a fly-by to the Moon may be included. In addition, in many papers such as in Quantius et al. (2012), the TLI is assumed to be performed at the perigee and tangent to the GTO (or phasing) orbit.

2. A mid-course maneuver supported by the Sun's gravity is performed once this region is reached. This maneuver should take the satellite to the Moon or to an intermediate supporting state. Here, due to the presence of large third-body forces, the required plane-change maneuvers can be included with no or very little ΔV. To calculate this maneuver so that its objective for ballistic capture is met (in Section 5.3.3), Quantius et al. (2012) uses a targeting sequence. This maneuver can be calculated using an algorithm that changes its value slightly in all axes.

3. As soon as the satellite arrives at the Moon, a lunar orbit insertion is required. This can be done through a single or split maneuver(s) until the final orbit is obtained. Quantius et al. (2012) explains how phasing orbits can also be included for lunar orbit insertion, as in the case for the Earth departure. Here, the lower the first periselene, the lower the required energy to achieve lunar orbit. However, it is also important to consider risk reduction, hence constraining the first periselene so that it is not too close to the Moon.

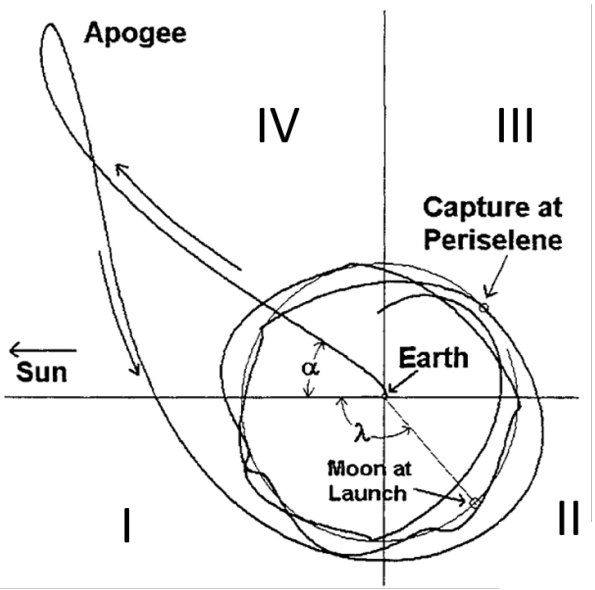

(a) Quadrant II WSB transfer in Sun-Earth rotating frame. Modified from Belbruno and Carrico (2000).

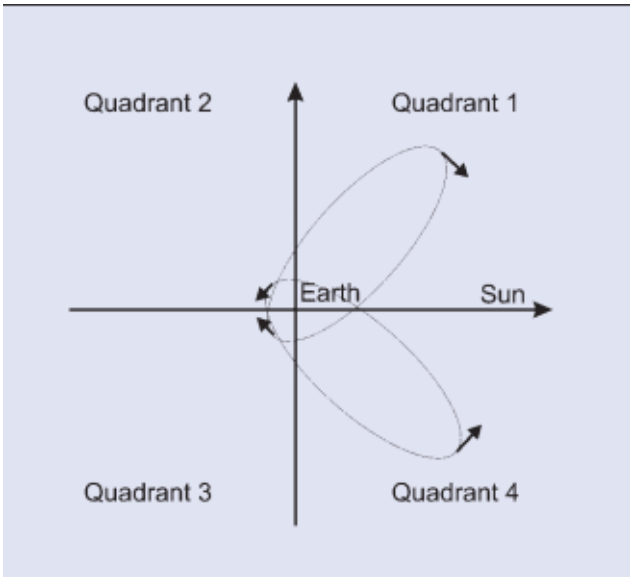

(b) Field-line directions of the Sun's gravity gradient in a rotating frame. The spacecraft is moving in the counter-clockwise direction. Retrieved from Biesbroek et al. (2000).

Figure 5.7: WSB transfer and quadrants for the Sun's gravity gradient directions. Even though the reference frames are different, the quadrants are labeled in the same way.

Figure 5.7 shows an example of a WSB transfer and the field-line directions of the Sun´s gravity gradient. According to Figure 5.7b, the orbital energy is only increased in quadrants 2 and 4, for which the gravity gradient is directed along the velocity vector at apogee, as the spacecraft is moving in the counter-clockwise direction. It has to be noted that the orbits shown in this figure are for easier understanding and visualization, but orbits plotted in a rotating frame will not be elliptical. Here, the orbital energy is increased, and integrating over the long period that the spacecraft spends in the apogee region, the perigee can be raised up to the Moon's distance. For these transfers, it is important to note the angle λ from Figure 5.7a, which denotes the Sun-Earth-Moon angle in the Sun-Earth rotating reference system.

Ariane's standard GTO is used as the initial orbit in many papers studying WSB transfers. Its line of apsides nearly coincides with its line of nodes, and it is directed towards the Sun-Earth line. In this orbit, the perigee is in the shadow of Earth. Starting the transfer to the WSB region at this perigee always requires a mid-course maneuver to be conducted in the Quadrant IV in Figure 5.7a, hence increasing the satellite's energy.

Many methods and reference systems have been used when calculating and optimising the WSB transfers. One way, explained by Belbruno and Miller (1991), is to integrate backwards in time from the Moon's orbit until a point within the WSB boundary region is reached. A second integration starts at a parking orbit around Earth and after giving a ΔV, integrates forward in time. Both integrations are altered so that the final positions of the transfer in the WSB region match, and the velocity mismatch is solved by a maneuver.

Another way to calculate these transfers is explained by Quantius et al. (2012). In his paper, the spacecraft is taken to the WSB region through an elliptical orbit with an apogee at 1.4 million km from Earth, where the mid-course maneuver was conducted. To calculate it, some supporting variables are added, including the angle γ between the Earth-Moon and the Earth-Spacecraft vectors, found in Figure 5.8. In the first perigee of the WSB return trajectory, this angle is constrained to approximately 4°, and the radial distance

between the Moon and the spacecraft is set to around 30.000 km. In this way, the spacecraft will fly slightly in front of the Moon, using its gravitational force to decelerate, decreasing the spacecraft's orbital energy to one similar to the Moon's. To ensure stable behaviour at perigee, Quantius uses a trick which consists of temporarily switching off the gravitational forces of the Moon from the point where the spacecraft crosses the plane generated by the Sun-Earth line and the ecliptic normal. This is done because these forces could disturb the target conditions. Nevertheless, it is important to take into account that this will lead to differences with respect to the real system, and hence, if used, this approach and its consequences should be further analyzed.

The main advantage of using this supporting condition is that it makes the code very robust, stable and autonomous. However, it restricts the solutions to non-optimized trajectories. As in the optimal solution, the apogee does not have to be fixed to 1.4 million km, and the supporting variables can be varied. Following this procedure, Quantius et al. (2012) was able to find a solution for every given launch date, but found problems where the inclination difference between the GTO and the Moon was at its worse (around 29°).

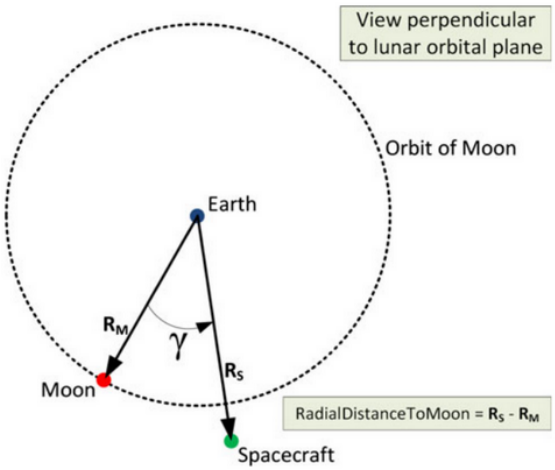

Figure 5.8: Example of supporting variables from Quantius et al. (2012).

Even though this approach gives a very robust solution that can be used for the development of WSB transfers, Belbruno and Miller (1993) explain that, in order to reduce the ΔV of a lunar transfer to its minimum, the hyperbolic excess velocity of Hohmann transfers needs to be removed. This is obtained by achieving a ballistic capture at the Moon following an invariant manifold of L_2, which gives, as found in Koon et al. (2001), an orbit that under the natural dynamics gets within the sphere of influence of the Moon and performs at least one revolution around the natural satellite. Here, a negligible amount of energy is required to stabilize the final elliptic orbit. In addition, the main mid-course maneuver will not need to be at apogee, but in the re-entry of the Earth's sphere of influence, at around 900,000 km. Hence the supporting constraint of Quantius et al. (2012) does not make sense if the most optimum solution is looked for. A more in-depth explanation of the ballistic capture is found in Section 5.3.3.

An additional way to calculate WSB transfers has been proposed and explained by Koon et al. (2001). The idea is to model the 4-body system using the patched-conics method, but approximating it as two coupled 3-body systems, following a similar idea to the patched-conic method used for direct transfers with 2-body dynamics, found in Section 5.1.1.

A comparison can be made between a WSB transfer and a direct transfer in terms of propellant saved. For instance, Zazzera et al. (2004) found that a WSB transfer between two circular orbits with altitudes of $h_E = 167$ km and $h_M = 100$ km has a total cost of $\Delta V = 3838$ m/s, which is 153 m/s less than a

Hohmann transfer. Nevertheless, Quantius et al. (2012) gives that the transfer time of a WSB transfer is in between 3 to 5 months depending on the launch epoch w.r.t. the Moon's position, compared to a time of flight of around 5 days of a Hohmann transfer. As the saving in ΔV is not substantial and the time of flight increases considerably, these transfers are usually considered for recovery of emergency conditions, as demonstrated by the Japanese spacecraft Hiten.

Moreover, to reach this distant WSB region in the Sun-Earth system, a lunar fly-by can be used, as it allows the spacecraft to gain sufficient energy, explained in Section 5.5. Parker and Anderson (2013) explains that for a typical WSB transfer, a Jacobi constant (C) of around -0.7 to -0.4 km^2/s^2 is required. Nevertheless, if a lunar gravity assist is included in the transfer, the C requirement can go down to -2 km^2/s^2.

When optimizing these transfers, it is important to consider that they take place in an extremely complex and chaotic environment, hence requiring methods that assure a global convergence at least to a local minimum, which is the main reason why most of the researchers choose an evolutionary process for the calculations. In addition, through a thorough analysis, Ockels et al. (1999) found that the leading parameters of the WSB transfer using a GTO as the initial orbit are the angle between the GTO's apsidal axis and the Sun direction, which in Ariane 5's case ranges from 6° to 20°. These highlights the effect that the timing in these transfers has on the optimization.

Lastly, when looking at WSB transfers, some challenges may come from a navigational point of view, as small errors in velocity may translate into large errors in the final position when propagating in the vicinity of the Lagrangian points.

5.3.3 Ballistic capture

As explained by Belbruno (2000), a capture trajectory is called *ballistic* if the energy of the satellite with respect to the Moon is negative ($E_{P,M} < 0$), implying that an extra maneuver for capture is not required ($\Delta V_c = 0$). These transfers including the ballistic capture were first numerically demonstrated by Belbruno (1987). In addition, Belbruno (2000) also gives an analytical explanation on how to calculate the distance r_M where a spacecraft orbiting the Moon will be between capture and escape, giving a way to numerically estimate the WSB around the Moon that allows for this ballistic capture. With $r_M = r_M(e_M, \theta, E)$, where e_M is the eccentricity about the Moon, and θ the angle between the x-axis of the CR3BP and the spacecraft.

In Belbruno and Carrico (2000), a contour plot giving the possible e_M for values of r_M close to zero is obtained. r_M needs to be close to zero as it is non-dimensionalized with respect to the Earth-Moon distance; in their examples, the values correspond to 500 km altitude from the Moon. The main conclusion reached is that there are many values of E, and hence of C, that will lead to ballistic capture. In their example, E ∈ [-3.12, -2.98]. In addition, it was found that the values obtained using the calculations from Belbruno (1987) agreed with the actual ballistic capture transfers, verifying the validity of the model.

The ballistic captures make use of the effects of the Earth-Moon WSB, hence requiring a 3-body decomposition of the Solar System, as the 2D decomposition does not explain the needed features. They target the invariant manifold of L_2. A sketch of these capture orbits is found in Figure 5.9.

It is important to note that the ballistic capture gives a highly unstable elliptical orbit in the weak stability region of the Earth-Moon system, hence requiring a stabilization maneuver. As found in Belbruno and Miller (1991), the orbit obtained has an eccentricity of about 0.94, and a maneuver of 30 m/s performed at periapsis should be sufficient for stabilization. It is also stated that an orbit with such an eccentricity should be enough for lunar observation. Nevertheless, much more propellant will be required to achieve a circular orbit. Therefore, when optimizing these kinds of orbits, the ΔV required to go from the obtained

orbit with ballistic capture to the needed LLO has to be considered.

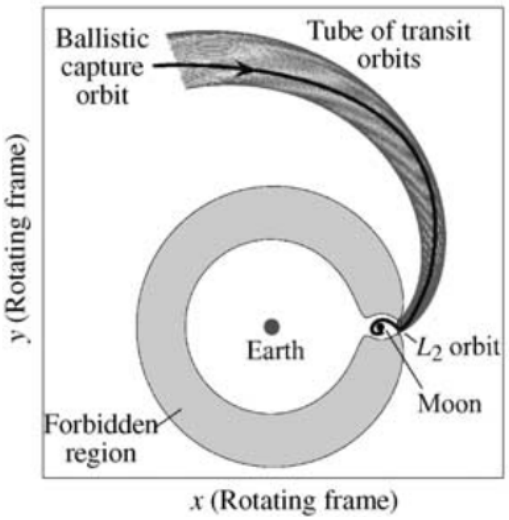

(a) Trajectories inside the stable manifold tube will transit from outside the Moon's orbit to the Moon capture region.

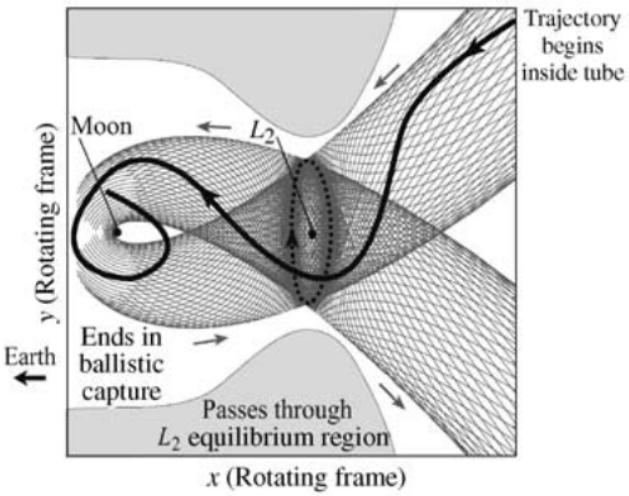

(b) Trajectory that ends in ballistic capture at the Moon.

Figure 5.9: Ballistic capture at the Moon. Retrieved from Koon et al. (2001).

5.4 Manifold transfers

As explained by K. C. Howell et al. (1994), manifold transfers are low-energy Earth-to-Moon transfers which make used of the stable manifolds in the CR3BP to reach the Moon; these manifolds and their calculations are found in Section 3.2.1. The main manifold used for these transfers is the one related to L_1, as these low-energy transfers through L_1 require the minimum energy to reach the Moon, as found in Figure 3.3. Nevertheless, as explained by Zazzera et al. (2004), it is important to highlight that not all trajectories that go through L_1 are low-energy transfers. In theory, assuming $C < C_1$, any direct transfer that goes through the neck opened at L_1 exists. Nevertheless, without using the invariant manifold theory, the design of these trajectories are very difficult due to the chaotic regime around the Lagrange points, giving an example of the benefits that this additional structure within the CR3BP provides.

As seen in Figure 3.5, the unstable manifold through L_1 and towards the Moon gets very close to it. Nevertheless, the stable manifold towards Earth never gets closer than approximately 0.35 Earth-Moon unit distances. Therefore, to reach it, two maneuvers are required: one to leave the Earth's orbit, and another one to obtain the conditions to inject into the stable manifold. On the other hand, as explained in Parker and Anderson (2013), the stable manifolds related to the Halo orbits in the Sun–Earth system intersect Earth, hence obtaining great advantages for transfers towards these Halo orbits using the manifold technique, as only one maneuver is required to inject into the stable manifold. Once in it, the spacecraft will asymptotically arrive at the target orbit.

These transfers are also specially interesting to get into one of the periodic orbits of the Earth-Moon system, because, as found in Section 3.2.1, these orbits also have manifolds related to each of their points. Parker and Anderson (2013) gives a procedure to obtain a direct, two-burn transfer to a lunar Halo orbit based on targeting states within the stable manifold. This procedure has been used for the design of missions such as Genesis, found in Lo et al. (2001). Firstly, the objective Halo orbit needs to be calculated. Then, the manifold segment related to one of the orbital points is generated by propagating backwards

in the direction of its stable manifold in the CR3BP. Next, the state in this manifold segment at which the spacecraft needs to arrive to inject to the manifold is defined. From here, the bridge segment that encounters the Earth's parking orbit is generated by defining a ΔV_M tangential to the trajectory and propagating backwards until the first perigee passage. Lastly, the ΔV_{LEO} to get into that bridge segment is calculated. An example of this transfer is found in Figure 5.10.

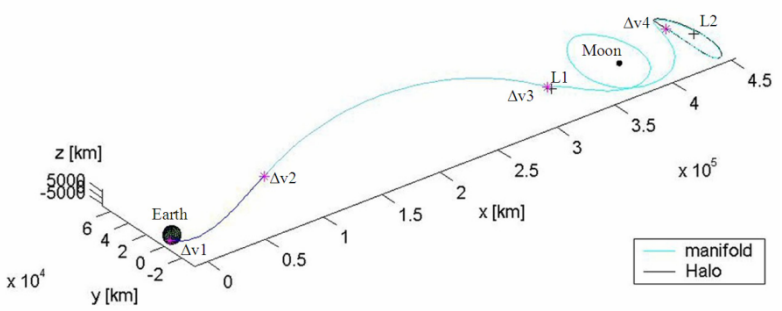

Figure 5.10: Manifold transfer through L_1 to an L_2 Halo orbit. Retrieved from Ceriotti et al. (2006).

There are two options to decide which point in the manifold to use. Firstly, the most intuitive way would be to start the manifold segment in the point of the manifold closest to the Earth, also called *perigee-point* scenario, as the energy change maneuvers are more effective when the spacecraft is travelling faster. The second option is to have an *open-point* scenario, where the point on the manifold is not chosen beforehand, leaving one more degree of freedom. In this case, it is important to generate the manifold for a larger period of time, for instance one month. Parker and Anderson (2013) found that this second case gives better results, hence reaching the conclusion that it is more efficient to perform a larger ΔV_{LEO} and a smaller, although less-efficient ΔV_{MI}. The main argument for it is that the maneuver at LEO can take advantage of its proximity to Earth, obtaining the total change of energy required as efficiently as possible. Nevertheless, for these cases, the transfer time may become larger, reaching values that are not of interest, hence a maximum allowable transfer time should be given. Parker and Anderson (2013) found that the most optimum transfer had a transfer time of 10 days, and the next of 22.7 days. Using the perigee-point scheme, a transfer time of 16.86 days was found. It is interesting to note that most energy-efficient solutions found perform their energy-changing maneuvers close either to Earth or to the Moon, making use of their gravity wells.

From these calculations, there are two aspects important to point out. Firstly, in most of the cases, it is assumed that the transfer will use only two ΔV's and that they will be tangential to the velocity direction. Nevertheless, there is no guarantee that this approach is the most optimum one, but it reduces the degrees of freedom considerably. Secondly, the results from other papers cannot be used for all the actual transfers to real Halo orbits, as their performance will vary based on the date and orientation of each body and its orbit in the Solar System.

5.5 Transfers with lunar fly-bys

A fly-by is a gravity-assist maneuver where the kinetic energy of a spacecraft is increased or decreased using the gravitational field of a body without the need of an extra maneuver. This technique has therefore become a common technique to save propellant in many space missions. One important aspect to consider in these maneuvers, as explained in Huckfeldt (2020), is that the conservation laws of momentum and energy are still present and hence the change in kinetic energy is only apparent in the heliocentric

representation. Due to the conservation of momentum, Equations 5.13 are obtained.

$$\begin{aligned} m_P\ \vec{v}_{P,i} + M_M\ \vec{v}_{M,i} &= m_P\ \vec{v}_{P,f} + M_P\ \vec{v}_{M,f} \\ \vec{v}_{M,f} - \vec{v}_{M,i} &= \frac{m_P}{M_M}(\vec{v}_{P,f} - \vec{v}_{P,i}) \end{aligned} \tag{5.13}$$

These equations show that a large increase of the spacecraft's velocity will yield only a very small velocity change of the planet because of the large difference in their masses. To calculate the effects that a flyby has on the velocity and energy of the spacecraft, the patched-conics model is typically used, and hence the gravity field of the flyby body is only considered if the spacecraft is inside its sphere of influence, and the effect of the gravity of the rest of the bodies is ignored.

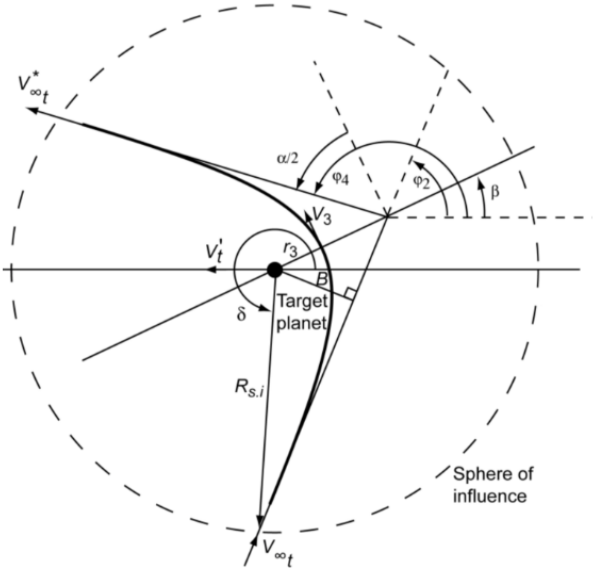

(a) Flyby geometry.

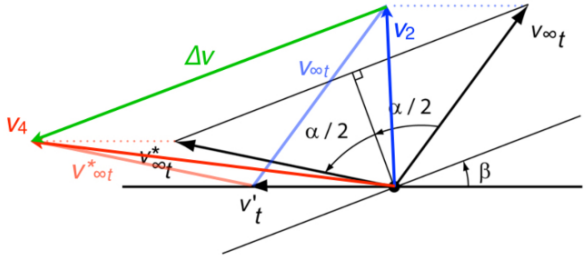

(b) Velocity diagram of a flyby.

Figure 5.11: Gravity-assist maneuvers diagrams of characteristic velocities and angles. Retrieved from Cowan (2021a).

The increase in velocity that can be obtained with a flyby is calculated using the diagram in Figure 5.11b and Equation 5.14.

$$\Delta V = 2\ V_{\infty t}\ \sin\left(\frac{\alpha}{2}\right) \tag{5.14}$$

$$\alpha = 2\ \arcsin\left(\frac{1}{e}\right) \tag{5.15}$$

with $V_{\infty t}$ being the velocity in the Moon's inertial reference frame that the spacecraft has when entering its sphere of influence. α is the angle between the initial and final velocities. These velocities have the same module, $|\vec{V_{\infty t}}| = |\vec{V_{\infty t}}^*|$

The change in total specific energy is then:

$$\Delta\xi = V'_t\ \Delta V\ \cos\beta \tag{5.16}$$

with V_t' being the velocity that the Moon has with respect to the ECI reference frame. And β is a flyby design parameter found in Figure 5.11a.

These approximations of 2-body dynamics have great advantages to obtain analytical first estimates of the effect of a lunar flyby. Nevertheless, the patched-conic model fails to include some phenomena that come with the three-body formulation. Therefore, some research has been done to model the fly-bys in the CR3BP. Liu et al. (2021) was able to develop a Gravity Assist Mapping based on Gaussian Process Regression that can quantify flyby effects in a full three-dimensional situation. His work is based on the studies of the Keplerian Map and Flyby Map, which where semi-analytical techniques that employ numerical methods to generate the solutions.

To conclude, the use of flybys is very helpful to reduce the launch energy requirement. Nevertheless, they include an increase in complexity that triggers an operational risk of the mission. Some example where flybys were successfully used are; the Cassini mission, Rosetta, New Horizons.

5.6 Comparison between types of transfers

Throughout this section, many types of possible transfers to follow towards the Moon have been analyzed. With the help of these analyses, a comparison between all the transfers will be conducted in order to decide which transfer is the best option for a thorough study in the master thesis project.

Direct transfers have many advantages, which is the reason why they have been greatly used in missions to the Moon throughout the years. Firstly, they have been carefully studied, and first-order approximations are already available. Secondly, the transfer time is short, offering benefits when looking at radiation shielding and the time for mission control and communications. In addition, the spacecraft stays within close proximity to either Earth or the Moon, hence the effect of the Sun's gravity is not required for a first approximation. Nevertheless, its main drawback is the large ΔV required to reach the Moon, which is directly related with the cost.

On the other hand, a bi-elliptic transfer also offers some advantages specially concerning the decrease in ΔV obtained when the inclination change is performed further away from the body. This maneuver is performed inside Earth's sphere of influence and hence the Sun's gravity does not have to be included as a first approximation. Nevertheless, its main drawback compared to a direct transfer is the longer transfer time.

It was found by Perozzi et al. (2008), that Hohmann transfers would require the minimum energy if the orbits are not too distant, but if the ratio R_2/R_1 is larger than 15.58 a bi-elliptic transfer would be more efficient. For lunar transfers, in most of the cases, the ratio is lower than that value. Even though for transfers with inclination changes a bi-elliptic transfer is more efficient, its benefits do not cover for the increase in transfer time, which is the reason why it has not been used by many real missions, and hence why it is not going to be considered in the master thesis project.

An advantage of direct transfers and bi-elliptic compared to WSB and manifolds is that the only important factor for the computations is the orientation of the initial orbit with respect to the final orbit, and in case of transfers to the Moon, the position of the Moon. However, WSB transfers also need the Sun to be in the correct position w.r.t. the other two bodies.

WSB transfers, specially when using ballistic capture, have shown substantial improvements in terms of ΔV performance compared to other transfers, as explained by Belbruno and Miller (1991). In addition, low-energy transfers have access to a much broader range of lunar orbits for a particular arrival date than direct transfers. It has to be highlighted, as explained by Villac et al. (2003), that a ballistic transfer offers higher benefits when transferring to periodic three-body orbits rather than to a Keplerian lunar orbit,

specially if the objective orbit is close to circular, as the extra ΔV required to reach it will also need to be considered, and the propellant saved is considerably decreased.

WSB transfers also have some drawbacks. The main one is the increase in the time of flight, which can range from 3 to 5 months when transfering from a LEO to a LLO, and that also increases the costs of the overall mission due to its longer duration. Nevertheless, for some missions, a longer time of flight is not detrimental, as it gives time to solve errors and conduct extra measurements. It is also important to highlight the effect of the radiation exposure due to the longer times of flight and the fact that the spacecraft will not be protected by the Earth's magnetic field. This fact make these transfers not suitable for human exploration, except if the objective is to demonstrate a long deep-space transfer. The radiation is also detrimental for the electronics, which should include thicker shielding, increasing the mass of the spacecraft.

Moreover, the chaotic environment around a WSB makes these transfers very sensitive to variations in initial conditions, complicating the optimization, requiring a high accuracy of the thruster in the mission, and a good analysis of the station-keeping maneuvers throughout the flight. Furthermore, to accurately model this region, complicated modelling procedures need to be derived and run on supercomputers due to the need of solving a complex multi-body problem. Nevertheless, the exact modelling of these regions may not be required for calculating the transfers. Lastly, as stated before and explained by Villac et al. (2003), the position of all three bodies in space and time is important in a WSB transfer, as it can greatly change the outcome of the optimization.

Manifold transfers have also been studied as an interesting low-energy option to reach the Moon; they exploit the dynamics of the CR3BP and allow for a decrease in ΔV, without, in general, a large increase in time, as is the case for other low energy options. Even though this procedure for the transfers has proven to bring many benefits, its main advantages come when transferring to a periodic or quasi-periodic orbit through their related stable manifolds. The main disadvantage of this method is that the CR3BP formulation is required, as manifolds cannot be found in an inertial frame.

After comparing all options for a lunar transfer, it has been decided that this project will focus mainly on direct transfers, as they are greatly used by the industry, they are reliable, and an optimization considering external perturbations can be conducted. Within them, the possibility of obtaining trajectories that include a flyby will also be considered. Due to the fact that the main focus of final orbits are Moon-bounded orbits and not periodic orbits, manifold transfers will not be considered in initial propagations. These transfers require the CR3BP formulation, and have been already studied by fellow students, such as Tatay, 2019. Nevertheless, it could be an interesting addition for future work.

5.6.1 Low thrust

As a final note, this project is going to focus on high-thrust transfers to the Moon, as solar electric propulsion spacecraft require different trajectories, which are mainly based on trajectories consisting on high number of spirals with increasing apogee obtained with continuous low-thrust arcs, until the satellite is at a sufficient distance to become captures by the Moon's gravity field. This will therefore require an optimal control problem solution instead of ΔV minimization, and a significantly grater transfer time.

Chapter 6

Current lunar missions

This chapter will deal with the most important and interesting lunar missions up to date, including the trajectories they followed to reach the Moon. In addition, a small market study of the current interests in the Moon will be performed in order to find which is the best way to deal with the optimization problem from the point of view of the users.

Literature shows that nearly a hundred spacecraft have flown to the Moon using conventional, direct transfers. On the other hand, only five have flown low-energy lunar transfers (WSB). Hiten and Artemis were able to extend their missions to the Moon despite not having enough propellant to reach lunar orbit using conventional techniques. GRAIL was the first to implement a low-energy transfer as part of the primary mission in 2011.

6.1 Past missions

The first missions to the Moon followed very quick transfers with lower than 1.5 days to reach the Moon, they sometimes involved lunar fly-bys, and had no intention of inserting into orbit. This section will include a recap of the Apollo missions and a brief description of Luna mission from the Soviet Union, Chang'e from China and Chandrayaan from India, all following direct transfers, as well as Hiten and possible student lunar missions.

Apollo

It is not possible to talk about past missions to the Moon without looking into the Apollo program, which was a 17-mission project conceived in 1960. Apollo-1 failed in 1967 during a simulation on the launch pad, and it was not until Apollo-7 that crew got into space. Apollo-8 became the first manned mission to orbit the Moon, and Apollo-11 took the first man to the Moon in 1969.

In the first four years of the program, an intensive study about the main trajectories to go to the Moon was developed. It was found obvious that, at that time, the most reasonable way to go to the Moon and back was using the circumlunar free-return trajectories, found in Figure 6.1a, which are also called figure-8 paths. These trajectories will go around the far side of the Moon at a perilune altitude of around 110 km and return to the Earth using the Moon's gravity and without the need of any extra propulsion. As explained by Berry (1970), by placing the spacecraft on this free-return trajectory, the crew had a way to return to Earth in case of any failure of the main command and service module engine. Depending on the distance from Earth to the Moon, the time of flight of these transfers ranges from 60 to 75 hours. The inclinations that can be obtained using these trajectories are within 10 degrees of the Moon´s equator.

Another option considered was the hybrid translunar trajectory, depicted in Figure 6.1b. Its name comes because it combines free-return and non-free return trajectories. Firstly the spacecraft is placed on a free-return trajectory but with a higher perilune that ranges from the 110 km altitude to several thousand km. Then, at approximately one day after TLI (usually before half way), the spacecraft conducts a maneuver that places it in another trajectory with the desired perilune of 110 km. Once in this trajectory, free return will not be possible without an extra maneuver. Nevertheless, it is possible to design these orbits in a way that return to Earth is feasible in case of failure, which is the reason why they were an option for Apollo. The main advantages of these transfers is that the possible ranges for time of flight are not as constrained, and hence can be used when the time of arrival at the Moon violates constraints such as lunar lighting or ground station coverage. In addition, the possible inclinations are also less constrained depending on the approach energy, minimizing the propellant required for LOI in some cases, and hence it is a good option when the free-return trajectory requires excessive propellant usage.

Due to the great sensitivity of the circumlunar trajectory to errors in initial conditions, mid-course corrections are typically required. In the Apollo-11 mission, four mid-course corrections were planned, nevertheless, only two of them were needed in the end.

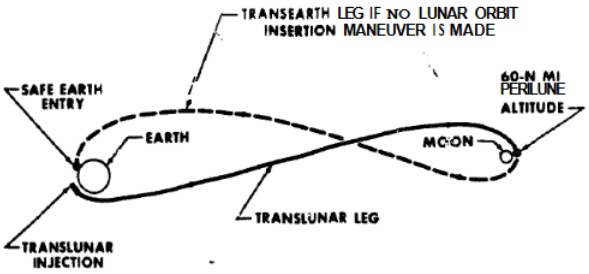

(a) Free return.

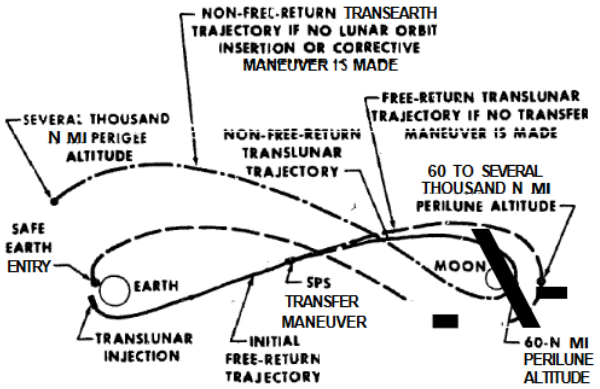

(b) Hybrid lunar trajectory.

Figure 6.1: Apollo launch options. Retrieved from Berry (1970).

Some data from the Apollo missions will be given to gain a clearer understanding of the characteristics of these transfers. Its initial parking orbit was at an altitude of around 190 km, and Apollo-11 took 73 hours to reach the Moon. Its ΔV budget given by Perozzi et al. (2008) was a $\Delta V_1 = 3.2$ km/s and $\Delta V_2 = 0.8$ km/s.

Luna

The Luna mission was conducted by the Soviet Union, with its first mission flying in 1959. Its last mission, Luna-24, was launched in 1976. Even thought Luna failed to take the first man to the Moon, it was able to conduct many *firsts*. For instance, the first spacecraft reaching escape velocity and to flyby the Moon with Luna-1, impact on the Moon, photographs of the far side, soft landing, lunar satellite, analysis of lunar soil, sample return, and the first lunar rover deployment. All its trajectories were direct transfers.

Chang'e

One of the nations with the highest increasing interest in the Moon is China, which has launched a series of lunar probes in their Chang'e satellites since 2007, with Chang'e 1 being the first Chinese spacecraft to travel beyond Earth's orbit. These missions are named after the Chinese Moon goddess. Their last mission to date has been Chang'e 5, a successful lunar sample return mission, launched in 2020. This

mission was tracked, for two of the missions' most critical phases, by ESA's ground stations. Chang'e 6 is scheduled for 2024 and two other missions are planed in the 2020s. All its missions up to date have followed a direct trajectory to the Moon, getting to a TLO for 5 days, where a number of trajectory corrections are performed and where solar panels are deployed.

Chandrayaan

Chandrayaan-1 was India's first mission to the Moon, and the beginning of the planetary exploration programme by the Indian Space Research Organization (ISRO). It was launched in 2008 and it was inserted into an elliptical lunar polar orbit. It took 11 payloads, four of them international and two being Indo-foreign collaborative payloads. A large volume of scientific data with excellent quality was obtained from the mission, allowing it, for instance, to find water on the Moon. Chandrayaan-2 was launched in 2019, planning to become the fourth country to land on the Moon, taking a rover to the lunar south pole. Nevertheless, just before touchdown on the Moon, the communications were lost. Both spacecraft followed direct transfers. Chandrayaan-2's orbit was progressively increased five times during 15 days until the TLI, taking it 6 days to reach the Moon.

Hiten

Uesugi (1996) explains that the main objective of Hiten´s mission, launched in 1990, was to orbit around the Moon to perform gravity field measurements and to demonstrate new technologies for planetary missions. This included to demonstrate orbit modification by means of aerobreaking in a planetary atmosphere. After its main mission was successfully achieved with 8 fly-bys, Hiten had 12 kg of propellant left, which corresponded to a maneuver ΔV of around 130 m/s. Hiten used a ninth swing-by to enlarge the orbital apogee to around 1.5 million km and hence be able to use the perturbation forces from the Sun in this WSB region. After flying on the orbit for 5 months, a tenth swing-by was used for Hiten to enter an orbit looping L_4 and L_5, and then encounter the Moon with a relative velocity that allowed for a maneuver within the spacecraft´s possibilities. Lastly, after almost two months in lunar orbit, the spacecraft crushed into the Moon due to the perturbations of Earth and the Sun, very close to the predicted point.

Student missions

Student missions are interesting for this project for many reasons. Firstly, student missions are backed by universities, which have a great interest in scientific research. Nevertheless, they require help from the industry. DLR being a German public institution is very interested in supporting these initiatives, and hence these missions could benefit from the software to be created.

European Student Moon Orbiter (ESMO): As explained by Ceriotti et al. (2006), this mission was part of Student Space Exploration and Technology Initiative (SSETI), a network of students and educational institutions supported by ESA whose main objective is to design, construct and launch micro-satellites and other spacecraft. The ESMO mission had as main objectives to take images of the Moon and transmit them back to Earth, to measure useful scientific lunar data, and to demonstrate the interplanetary micro-satellite concept. It was going to be launched as an auxiliary payload, using high-thrust impulsive maneuvers.

In March 2012, the ESMO project passed its Preliminary Design Review. However, although the review board was confident that the mission's objectives could be met, ESA's Education Office announced that the project was not going to continue to the next phase, as it was not sustainable within their budget constraints.

Other missions that served as educational outreach have also been studied, including the Lunarsat mission, the Hevelius mission, LUMIO, which is a CubeSat mission to a halo orbit at Earth–Moon L2, and even Lunar Zebro, driven by TU Delft.

6.2 Current missions

Artemis

The Artemis program is a both robotic and human Moon exploration program established in 2017, and led by NASA but conceived with the help of ESA, JAXA and CSA. As found in M. Smith et al. (2020), in March of 2019, the Vice President from the USA announced a new goal for NASA's human exploration campaign: to land the first woman and the next man on the lunar south pole by 2024, setting an ambitious deadline to the mission.

The Gateway is a spaceship that is going to be placed in a NRHO around the L_2 point of the Moon, and it is intended to stay there for more than 10 years. It is a very important part of the Artemis mission, as it will provide essential support for long-term human return to the lunar surface, giving the astronauts a place to live and work, and at the same time serve as a staging point for deep-space exploration. It will be made out of the Power and Propulsion Element (PPE), the Habitation and Logistics Outpost (HALO), and logistics services, all of which will be launched by Commercial Launch Vehicles (CLVs). The establishment of the Gateway will be a common effort with commercial and international partners. For the European part, a European Large Logistics Lander (known as EL3 or Argonaut) is being developed. Its main goal is to have a generalised lander capable of delivering a wide variety of cargo to and from the surface of the Moon and to and from the Gateway station.

As explained by M. Smith et al. (2020), the Artemis program includes two phases. Phase 1 achieves the new goal set by 2024. For it, two Gateway components are required; the PPE that will launch in 2022, and the HALO, a minimal habitation capability. After they are in place, Orion will take four crew members to the Gateway, two of them will remain on the orbiting command module, and the other two will take a commercially provided human landing system (HLS) in order to descent to the lunar south pole and and to get back to orbit afterwards. Phase 2 will focus on advancing the technologies to foster a continuous and sustainable presence on the Moon, making the lunar expeditions more affordable, and creating a sustainable economy on and around the Moon. Lastly, the programme also intends to create an Artemis Base camp on the surface of the Moon which would include a modern lunar cabin, a rover, and a mobile home, in order to give astronauts a place to live and work on the surface of the Moon.

In addition to all of this, the Artemis programme will create multiple side missions planned to sustain the Gateway, including many cargo missions.

The launch of the Artemis-I spacecraft the 16^{th} of November 2022 has become the first milestone of the program. It is taking the Orion spacecraft, designed to carry humans, around the Moon. It will follow a direct transfer, perform a lunar flyby and reach its closest approach the 21^{st} of the same month. After more than 25 days in deep space, Orion capsule has splashed down in the Pacific Ocean on December 11^{th}, completing its mission.

6.3 Future missions

Circi et al. (2006) gives a way to achieve lunar spacecraft constellations using WSB trajectories and hence obtaining relevant savings in ΔV. These studies can open the path to new missions that may require the calculations of WSB transfers. For instance, ESA has started an initiative called **Moonlight** with the aim of developing a constellation of satellites in lunar orbit able to provide connectivity and navigation services for all kinds of lunar missions. ESA believes that sharing these services between the space agencies would significantly reduce the costs and the design complexity of the future lunar missions. The study contracts for this initiative were awarded, in June 2021, to two industry teams led by Surrey Satellite Technology (SSTL) and Telespazio. Moreover, SSTL has already designed the **Lunar Pathfinder**, due

to launch in 2025, which will offer S-band and UHF links to lunar assets on the surface of and in orbit around the Moon, and an X-band link to Earth. Its main aim is to offer an affordable communication service. Moonlight's initiative plans to apply the lessons learned from operating the Lunar Pathfinder.

Blue Origin, a private US company founded by Jeff Bezos (also the founder of Amazon) in 2000 is currently looking towards the Moon, following the main paths of current space exploration. As explained in BlueOrigin (2022), Blue origin is working on a lunar module called **Blue Moon** as well as on the super-heavy **New Glenn** launcher, with a reusable first stage. Its main objective is to create an Amazon-like delivery service for the Moon, and be able to land on the south pole of the Moon in order to support the construction of a base there.

Google Lunar XPRIZE (GLXP), was a prized space competition organized by the X Prize Foundation, and sponsored by Google. XPRIZE is a non-profit organization that creates public competitions in order to encourage technological development that benefits humanity. From 2007 to 2018 a lunar competition was held for private companies, with a price of US$30 million, if they could land a rover on the Moon, travel 500 meters, and transmit back to Earth high-definition video and images. Unfortunately, no company was able to complete the challenge, but SpaceIL was awarded with US$1 million for reaching the Moon even if its spacecraft crushed on its surface. These initiatives will continue to appear as the Moon race advances. Even though no company was able to win the prize, many were created. For instance, PTScientists, a German company based in Berlin was founded in 2008 for the competition. In 2019, the company filed for bankruptcy, but in 2021 they won a contract with Ariane Group to build ESA's ASTRIS kick-stage, which would increase the versatility of Ariane 6 and enable new mission profiles such as missions to the Moon and/or deep space, reducing the spacecraft complexity and the risks inherent in orbit injection. Although this is their main current aim, their final objective is to conduct their our own commercial space exploration missions, including missions to the Moon.

In Germany, companies are also getting involved in this new phase of lunar exploration. For instance, OHB Systems has partnered with Israel Aerospace Industries to develop the **Lunar Surface Access Service** (LSAS), designed to become 'the first European Moon shuttle service'. It is planned to be launched in 2025, becoming the first European company to launch a commercial mission to the Moon

Chapter 7

Integration and propagation

As analytical solutions for the problem at hand can not be directly computed, numerical integration and propagation will be required. To be able to do so, a model that best represents the complete dynamics of the system is needed. Nevertheless, it is also important to consider the available resources, which include the computational capacity, the available data and its accuracy, and the CPU time. Therefore, it is important to understand the requirements of the project and the needed accuracy of the solution.

When looking at an optimization, many function evaluations will be required to obtain the best optimized solution, therefore, the accuracy and the running time of each function evaluation is something to consider. It is therefore key to look into the integrator and propagator that are going to be used, as these aspects are highly influenced by them.

In addition, the main programming language of this project is Fortran, a programming language that has been used by the Flight Dynamics team in DLR for many years. Therefore, another key aspect to consider are the in-house tools that have been generated, tested, used and improved by DLR throughout the years, which will be exploited in this project. This decision is specially important when looking at the integrator and propagator to use, because even though other integrators could be programmed, it would be out of the scope of this project and not beneficial due to the lack of time and real testing required for it to be used for operational purposes in real missions. Nevertheless, other programming languages such as python will also be used.

Firstly, it has to be noted that the actual requirements in accuracy have not been set by the team at the moment. But it is important to consider that the requirements for position and velocity set for the physical model drive the ones for the numerical model, which has to be 1 or 2 orders of magnitude lower to account for other error sources. For the case of the velocity, it is common use to set the accuracy to a percentage of the velocities that are looked at, for instance, 0.001 %. To calculate the error of the model used, a benchmark would be required, and shall have an error of 2 to 3 orders of magnitude lower than the numerical model. In addition to the physical and numerical requirements, the most important one to consider is the CPU time per run, as many runs will be required for a complete optimization, and the resources available are limited.

7.1 Integrator

First of all, some of the main integration options will be briefly explained. An integrator can be either single-step or multi-step, and they can be fixed-step or variable-step integrators.

A single-step integrator, such as Euler¨s method, only refers to one previous point and its derivative

to determine the current value. On the other hand, multi-step methods such as the Adams-Bashforth method, reuse the information of previous function evaluations to gain efficiency, referring to previous points and their derivatives. Lastly, there are other methods such as Runge-Kutta, which do not use previous information but take some intermediate steps to obtain a higher-order method. As explained by Cellier et al. (2006), in general, multi-steps algorithms offer a higher accuracy using only a single new function evaluation per step, hence allowing for a more efficient use of computational resources. Nevertheless, this is not always the case because it typically needs a smaller step. In addition, the interpolation between steps is easily derived. One of the drawbacks is that these methods require an initialization typically obtained by some data points with a very small time step, but this can bring some errors. The order of the method depends on the number of previous points considered.

On the other hand, there are fixed-step and variable-step integrators. As the name implies, a fixed-step integrator solves the problem at regular time intervals from the beginning to the end of the simulation, the step size chosen needs to be the smallest to get the required accuracy throughout the whole simulation. In general, decreasing the step size will increase the accuracy, but at the same time it will increase the time required to solve the model. On the contrary, variable-step algorithms vary the step size during the simulation to meet with the specified accuracy. When the model is under rapid dynamics, the step size is decreased, and when the states are changing slowly, the step size is increased to avoid taking unnecessary steps. In these algorithms, the step size needs to be calculated at each step adding a computational overhead. In many cases, the variable-step size algorithm shortens the simulation time for the problem significantly, specially if the dynamics of the system are changing. For the case of a lunar transfer, a variable-step size integrator is more suitable because the change in the dynamics is highly dependent on the proximity of the spacecraft to the primaries.

The integrator that is going to be used in this case, and that is already implemented in the DLR functions is **a variable-order variable-step size Adams-Bashforth-Moulton method** which is able to support a dense output by interpolation, explained by Shampine et al. (1976). The method uses a modified divided difference form of the Adams predictor-corrector (PECE) formulas and local extrapolation, which improves absolute stability and accuracy. It is able to adjust the order and step size to control the local error. In addition, it is able to control round-off errors and to detect when the user is requesting too much accuracy for the machine's precision, as explained by Watts et al. (1986).

The Adams-Bashforth-Moulton (ABM) method combines the Adams-Bashforth method, which is explicit, and the Adams-Moulton method, which is implicit. An implicit method cannot be solved directly, hence the PECE approach is used. Firstly, the explicit method is used to estimate $\bar{y}(t_{n+1})$, this is the predictor part found in Equation 7.1. Then, this value is used to evaluate the implicit method, called corrector and found in Equation 7.2. The optimal step size, which is only increased and decreased by an integer number to keep the method efficient, is calculated by estimating the truncation error comparing the predictor and the corrector. This algorithm will try to find the most efficient choice of order/step size by varying both the step and the order.

$$\bar{y}^{*}\left(t_{n+1}\right)=\bar{y}\left(t_{n}\right)+\Delta t\sum_{j=0}^{s}b_{j}f\left(t_{n-j},\bar{y}_{n-j}\right) \tag{7.1}$$

$$\bar{y}\left(t_{n+1}\right)=\bar{y}\left(t_{n}\right)+\Delta t\sum_{j=0}^{s}c_{j}f\left(t_{n-j},\bar{y}n-j\right)+c{-}1f\left(t_{n+1},\bar{y}_{n+1}^{*}\right) \tag{7.2}$$

In addition, the code requires a relative error tolerance (ϵ_r) for local error examination, which is set as a global parameter at 10^{-14} and an absolute error tolerance (ϵ_a) for absolute error test, also set as a global parameter to 10^{-10}. These values would ensure an accuracy of 1 cm for an integration of transfer orbit

for a period of 4 days. However, they will be studied and confirmed for the actual model, as they can be tuned depending on the application. Then, at each step, the code requires that:

$$|local\ error| <= |\bar{y}| \cdot \epsilon_r + \epsilon_a \tag{7.3}$$

7.2 Propagator

A decision on which propagator to use also needs to be made to increase as much as possible the accuracy of the numerical model also considering the computational time. Nevertheless, it has to be understood that, for a perfect integrator scheme, the propagator does not matter from the point of view of the accuracy. However, as the integrator introduces errors, the propagator does have an effect. There are several formulations for the propagators. These include Cowell, Encke, Kepler elements, Modified Equinoctial Elements or Unified State Model.

The formulation of the equations of motion for a general propagation scheme is the following:

$$\frac{d\vec{x}}{ds} = \vec{f}(\vec{x},\ s;\ \vec{p},\ \vec{u}) \tag{7.4}$$

where $\vec{x}$ are the state variables, s the independent variable (which is usually time), $\vec{p}$ the environmental parameters, and $\vec{u}$ the control parameters.

A Cowell propagation propagates the Cartesian states using the familiar formulation found in Equation 7.5.

$$\ddot{\vec{r}} + \frac{\mu}{r^3}\vec{r} = \frac{\sum \vec{F}_{pert}}{m} \tag{7.5}$$

$$\vec{x} = \begin{pmatrix} \vec{r} \\ \dot{\vec{r}} \end{pmatrix} \qquad \dot{\vec{x}} = \begin{pmatrix} \dot{\vec{r}} \\ \ddot{\vec{r}} \end{pmatrix} \tag{7.6}$$

where the central body's acceleration and the perturbations are treated separately. Cowell's formulation is straightforward, with simple equations of motion. Nevertheless, it can lead to large numerical errors due to the large values for the state derivatives. In addition, the elements follow large variations, making it more complicated to adapt the time step. To try to deal with these disadvantages, other methods were developed using different assumptions and knowledge of the system. For instance, Encke's formulation exploits the idea that the orbit will remain close to the Kepler one, hence calculating this reference analytically and only propagating the small deviations. The main disadvantage of this method is that, after a long propagation, the deviations become of the same order as the state, loosing its advantage and adding complexity to the differential equations. It is then a good option when it is known in advance that the orbit will have minor deviations from the initial Kepler orbit. Kepler elements are very useful, but bring singularities for near-circular and near-equatorial orbits. Therefore, the Modified Equinoctial Elements are reformulated Kepler elements to prevent most of these singularities. Lastly, the Unified State Model gets rid of nearly all the singularities, by using three parameters based on the velocity hodograph for two-dimensional orbits and quaternions or Modified Rodrigues Parameters to represent the orientation.

After this brief summary, it was found that, for highly perturbed motion or motion that can get close to some singularities, the Cowell propagator is the most competitive, as the rest of the methods loose their advantages.

It would be very interesting to conduct an analysis on the different propagator and integrators together. Nevertheless, for models like the CR3BP, many of the other formulations are discarded because the trajectory does not follow an orbit with a shape similar to a Keplerian one. In addition, Cowell offers

simple equations of motion and the simple and direct interpretation of the results, hence the **Cowell propagator** will be the chosen one.

Chapter 8

Optimization

Throughout this section, an analysis of the main optimization strategies will be included in order to decide which optimizer best suits the problem at hand and which one is best to study in the follow-up research. To do so, it is important to understand the problem, which has been done in the previous sections, but also to get a first idea on how it could be formulated, specially focusing on the most interesting objectives for the optimization.

The choice of optimizer is a very important step that needs to be taken with care in order to facilitate the work, get better results, or obtain the required robustness. Before making a decision of the choice of optimizer it is important to understand that the perfect optimizer for all problems does not exist, and that many things need to be considered, including the available literature and heritage.

An optimization consists on minimizing or, in some cases, maximizing a given function by changing the decision variables under some constraints. Obtaining a mathematical description of the problem as given by Chong et al. (2013):

$$\begin{aligned} & min/max\ f(\vec{x}) \\ & x_i^{(L)} \leq x_i \leq x_i^{(U)} \qquad i = 1, 2, ...I \\ & \text{subject to:} \\ & \qquad h_j(\vec{x}) = 0 \qquad j = 1, 2, ...J \\ & \qquad g_k(\vec{x}) \geq 0 \qquad k = 1, 2, ...K \end{aligned} \tag{8.1}$$

Where f represents the objective function, $\vec{x}$ is the vector of the design variables, h the equality constraints, and g the inequality constraints. J should be lower than I, but K may be larger. In an optimization, there could be multiple local minima and maxima, but only one global optimum, which is the objective result. It is also important to understand that the optima could be located in the limits of the design region - not good for robustness. In addition, not all problems in the design region have continuous derivatives, which is a problem for numerical methods.

An optimization has thee important parts, as found in Equation 8.1. They are the decision variables that are going to be used, the constraints, and the optimization objectives. These objectives are included in the function to optimized, which is called the cost function, and may include a system of penalties based on the constraints. Deciding the most optimum and interesting design variables and constraints will be part of the master thesis project.

8.1 Optimization objectives

Many optimization objectives can be considered when computing a lunar transfer. The main ones to examine are the time of flight (TOF) and the propellant consumption, which is typically expressed as ΔV so that the parameters of the rocket engine are not required. Nevertheless, there are also other possible objectives which could be useful for some applications such as number of maneuvers, eclipse time or ground station coverage. The two main optimization possibilities will be briefly explained in this section.

There are two ways to deal with the optimization objectives. The first one is to focus only on one objective, becoming a so-called single-objective optimization, and leaving aside other possible considerations or including them as penalties in the same objective function f, found in Equation 8.1. On the other hand, the problem can be studied considering different objectives, and hence a multi-objective optimization will be required. Both possibilities will be briefly explained below.

8.1.1 Main optimization objectives

Time of flight

The TOF is one of the most important objectives when looking at specific missions, specially those where the radiation reduction is important or where the time is a key factor. For instance, manned missions or emergency missions. Nevertheless, there are many other missions where the reduction of the time of flight, even if it is desired, it is not a key factor that needs to be optimized, just preliminary considered.

Propellant consumption

The propellant required for the maneuvers of the transfer is directly related to the mass of the satellite, as it will have to carry it since launch. The lower this mass is, the lower the launch costs, or the higher the mass that can be used for the payload. Therefore, reducing the propellant consumption in a transfer will always be an objective to consider.

In this work, and as concluded in Chapter 4, the initial state will be the initial Earth-bounded orbit, and hence the optimization will not include the ΔV required for the launcher to get to the initial orbit, as it is not part of the scope of the project.

8.1.2 Single-objective

In a single-objective optimization problem, the design variables will be optimized to reduce as much as possible the defined objective function. This objective function will include mainly one of the objectives explained before. However, there are other ways to deal with additional objectives in order to include them in some way in the optimization. For instance, the objective function can be defined including a penalty function, they can be added as a constraint, or as a maximum allowable value. The main advantage of a single-objective optimization is a single solution will be obtained as the output.

8.1.3 Multi-objective

With multi-objective optimization, many different objectives can be analyzed at the same time. However, it is important to take into account that, typically, these objectives are opposing ones, meaning that reducing one leads to an increase in the other. For example, a decrease in the propellant consumption, specially when looking at low-energy transfers, will, in most cases, lead to an increase in TOF. Therefore, there will not be a single solution, but a so-called Pareto front of the most optimal solutions from which

to choose. This Pareto front is easy to visualize for two objectives, but can become very complicated when considering three or more objectives. It is also important to highlight that this optimization is more complicated and some optimization techniques can not be used.

8.1.4 Optimization objectives comparison

Even though multi-objective optimization is a good way to incorporate two different, and in general opposing, objectives important for all transfers, it is found that the complexity that it brings and the decision that the user needs to make in the end is not of interest. Moreover, single-objective optimization can include different considerations by modelling the objective function in an intelligent manner using, for instance, penalties. In addition, the user will have a clear idea of its main objective before-hand, and hence will look for a single solution that satisfies it. Therefore, the decision taken for this project is to make a single-objective optimization but considering other factors using penalty functions that can be modelled by the user. Due to the time restrictions, the modelling of these objectives is going to focus only on TOF and propellant consumption. Nevertheless, for future work, other objectives and constraints such as number of maneuvers or ground station coverage could be included.

8.2 Optimization algorithms

There are many ways of categorizing all the possible optimizers that can be used for the problem. For instance, an optimizer can be global or local. Local optimizers can typically handle a small search space within the function to be optimized $[f(\vec{x})]$. Nevertheless, as explained before, this function can have many minima, but only one will be the global optimum. For these local optimizers to obtain the global optimum, a good initial guess is required. On the other hand, global algorithms try to deal with this problem in different manners, however, even with these global methods, there is no guarantee that they will converge to the global minimum.

Even though this distinction is very important to understand the different optimizers, the main way to categorize them is in gradient-based and Evolutionary/Genetic algorithms. The latest two follow different approaches but can be explained together. Due to the availability of the software in Fortran and the fact that they have been tested and used for different projects within the DLR group, one specific optimizer for each subgroup will be looked at in more detail. They are the SLLSQP as a gradient-based algorithm, and PIKAIA as a genetic algorithm. Moreover, a last approach combining both options and called a hybrid algorithm will also be explained.

8.2.1 Gradient-Based Optimization

These optimizers rely on the derivatives of the objective function $f(\vec{x})$ calculated either analytically or numerically to find the best combination of decision variables $\vec{x}$ that lead to the most optimum result. These derivatives can be expressed with the gradient, the Jacobian or the Hessian matrices depending on the order of the method used and the number of design variables. They are mainly used in convex functions, and can get increasingly complicated when dealing with non-linear functions.

One of the main advantages of the gradient-based optimization is that, given a good initial guess, the method will converge to the global optimum. Furthermore, it is easy to establish the search direction, hence the convergence is quicker than evolutionary and genetic algorithms, as they take advantage of the previous knowledge of the problem. Moreover, they have been greatly studied and are very well understood.

Nevertheless, they also have some disadvantages. For instance, if the initial guess is not close enough to the solution, the global optimum may not be found. Moreover, it can not deal with the optimization of functions that have a large number of local minima (multi-modal functions) or with functions with discontinuities.

SLLSQP

SLLSQP is a Sequential Linear Least SQuares Programming algorithm designed to solve general non-linear optimization problems. The optimizer approximates the non-linear function around the current guess using linearized least squares, and then finds the direction of greatest descent with the calculated gradients and a system of jumps, dividing the problem in many sub-problems, as explained by Horn et al. (1983).

This optimizer has been greatly used by the DLR team, and therefore is well known. In addition, it has proven to work correctly with similar software, which is the reason why it will be the chosen one if a gradient-based optimization is selected. Nevertheless, is important to take into account that the function and the constraints need to be continuous, and that it is a local optimizer, meaning that it may lead to a local minimum if the initial guess is not chosen correctly.

As this optimizer has been used before in a previous software, a diagram of the way the optimization works is given in Figure 8.1. Firstly, the initial guess for the design variables (also called decision vector) P is required. From there, FUNDER is called, where the scaled decision vector (P_S), the cost (V) and the constraint vector (G) are calculated, and are taken as inputs for the optimizer.

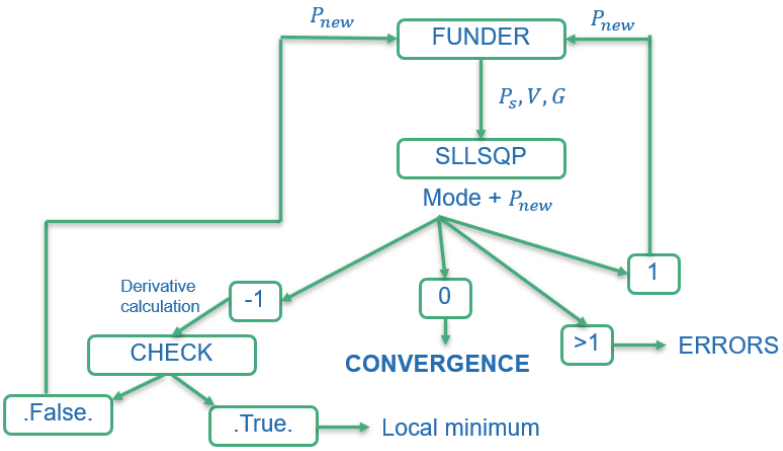

Figure 8.1: Optimization diagram.

The SLLSQP optimizer will give the new decision vector (P_{new}) and the mode. The mode decides the next steps. With mode 1, the given P_{new} will be used for the new calculations and as inputs for the SLLSQP. With mode -1, the derivatives will be calculated again for a gradient evaluation where checks are performed to see if the change is big enough to continue the optimization or if a local minimum has been found. If not, the process starts again. If the mode is larger than 1, the optimization will be stopped because an error has occurred. The most common errors are: mode = 6, meaning that a positive directional derivative has been found, and mode = 8, meaning that the iteration count has been exceeded. If one of the error modes appears, it is very useful to check the optimization parameters, like the accuracy or the weights. Lastly, the optimization will be finished when the output mode is 0, meaning that convergence has been reached.

The SLLSQP optimizer can handle equality and inequality constraints. The inequality constraints have

as a general formulation: $F(\bar{z}) \leq \bar{b}$. Nevertheless, when adding them as inputs to the optimizer, they need to be expressed as $F(\bar{z}) - \bar{b} \leq 0$. For the case of the equality constraints, the input should be expressed as $F(\bar{z}) - \bar{b} = 0$.

8.2.2 Evolutionary Programming and Genetic Algorithms

The evolutionary and genetic optimizers, as explained by Vikhar (2016), are global search algorithms inspired from the biological process of evolution by means of natural selection, also called *survival of the fittest*, hence they are both evolutionary algorithms. Mooij et al. (2022) explains that it strategically searches the whole design space by creating a population with N individuals of guesses of design variables. Each of them are evaluated and a fitness (a measure of the goodness of fit) is assigned to each of them. Then, a subsection of the initial population, called *parents* (in general, with the highest fitness values) is selected and recombined to create a new population (*offspring*) also with N individuals which are again evaluated. This procedure is repeated until a termination condition is reached. Due to this fitness values, in each iteration, the algorithm will focus more in the most promising areas of the design space, following, in general, natural processes such as the flocking of birds searching for food (Particle Swarm Optimization), or the pheromone trails used by ants to find the shortest path between their nest and food (Ant Colony Optimization).

The difference between genetic algorithms and evolutionary programming is that, for genetic algorithms, the independent variables are binary coded. In evolutionary programming, the independent variables are real numbers, hence changing the way the recombination of the population (mutation) is conducted. Using real numbers gives evolutionary algorithm the advantage of having better accuracy and faster convergence.

The main advantage of these algorithms, as found by Goldberg (1989), is that they are not limited by the objective function or the design space characteristics. This is because, as they are not gradient-based, they can handle discontinuities, non-linearities and multi-modal functions. Moreover, these algorithms will search throughout the whole space, and hence the initial guess is not determinant to reach the global optimum.

Nevertheless, they also have some drawbacks. For instance, as explained before, and even though these methods are global algorithms, there is no guarantee that they will converge to the global optimum, as they depend on random heuristics and because the solution is "better" only in comparison with the other solutions. Moreover, there is a large increase in computational time compared to gradient-based methods. This is because the model will need to be evaluated many times, computing new individuals and their associated goodness of fit for every parameter set. If this evaluation is computationally expensive, this approach can become impractical. Genetic algorithms are more computationally manageable because they reduce the number of function evaluations.

PIKAIA

As explained in *PIKAIA* (2022), PIKAIA is a function optimization subroutine for Fortran based on a genetic algorithm. This subroutine has been proven to be very robust and useful for multi-modal optimization problems, with global minima but also local minima. It was developed by a scientific division of the National Center for Atmospheric Research (NCAR) in Boulder, Colorado, and it is open source.

This routine **maximizes** a Fortran function given by the user. This is important to consider, but it can be seen that a maximization is a minimization with a minus sign. Moreover, the genetic operators used in PIKAIA are uniform one-point crossover, and uniform one-point mutation. In addition, three reproduction plans are available; Full generational replacement, Steady-State-Delete-Random, and Steady-State-Delete -Worst. In the default option, elitism is used, which helps to keep the reference of the promising areas of

the search space through the generations. In addition, the default option also gives a way to dynamically control the mutation rate by monitoring the difference in fitness between the current best and median in the population. The selection phase is rank-based and stochastic, and it uses the Roulette Wheel Algorithm.

The PIKAIA optimizer has not been used by the author in previous projects, so the way it should be formulated, obtained in *PIKAIA* (2022) will be given:

$$\text{call pikaia}(ff, n, ctrl, xb, fb, status) \tag{8.2}$$

where *ff* is the Fortran function to be maximized, defined as *function ff(n, x)*, and that gives a positive-definite measure of the fitness associated with point x that has to be inside the search space. n is the dimension of the search space (given in *dimension x(n)*). *ctrl* is the control vector whose elements determine the behavior of the algorithm. Its built-in default values have proven to be robust. xb is the optimal solution defined as the best solution in the final population at the end of the evolution. fb is the fitness of the solution, given as a scalar number from $ff(xb)$. The *status* gives either successful termination or error conditions associated to illegal input parameters.

8.2.3 Hybrid algorithms

Hybrid algorithms consist of the combination of a global search by an evolutionary algorithm and a local optimization by Sequential Quadratic Programming (SQP). Ceriotti et al. (2006) explains that solutions can be generated with a genetic algorithm able to search the whole space and find a feasible solution close to the global optimum, and then refine the solution by using it as an initial guess for a gradient-based algorithm.

8.2.4 Comparison of optimization algorithms

As explained before, it is found that a gradient-based algorithm brings many advantages including a fastest convergence, the assurance that with a good initial guess the global optimum will be obtained, the use of the previous knowledge of the problem, and the grand number of studies and information found about them. This is also the case for the SLLSQP optimizer, which has been used by the author in previous projects, adding a valuable insight. On the other hand, a genetic algorithm like PIKAIA is able to look through the whole search space without the need of a good initial guess, and can deal with non-linearities, discontinuities, and multi-modal functions.

The main disadvantages of a gradient-based optimizer are that, if a good initial condition is not given, the global optimum may not be found. Moreover, the functions to evaluate need to be defined in a way to avoid discontinuities, adding a significant amount of complexity to the problem. On the other hand, genetic algorithms can not ensure that the exact global optimum has been found, and they are computationally expensive, specially if a high accuracy is expected.

It is found in many papers, for instance in Zazzera et al. (2004), that systems with chaotic dynamics make using a gradient-based optimization very complicated or even impossible, as natural discontinuities need to be avoided when modelling the optimization. This is even more true for WSB trajectories, which are highly dependent on the initial conditions and go through a very chaotic region. It is also the case when using the CR3BP, as the transfers follow an irregular behaviour with a very sensitive dependence on the initial conditions hindering the long-term predictions of the state of the system.

A fine solution that includes many perturbations is required for this thesis. Therefore, a solution found

using a gradient-based optimizer is desired. Nevertheless, a hybrid method will be used, as the initial guess for the gradient-based optimizer will be calculated using a genetic algorithm that can deal in an easier way with the chaotic dynamics of the problem.

Chapter 9

Validation and verification

One important part of a project concerning the programming of a simulation and optimization software is the validation of such software. This is going to be looked at in more detail during the master thesis, as more information will become available.

For validation several things can be done. Firstly, as some optimizations have been conducted in previous research, data obtained by them always using their same specifications could be used for comparison. A refinement with a gradient-based optimization including a full dynamical model is not typically included, and hence would need to be discarded for the comparison. In addition, the minimum ΔV_{tot} can be calculated, as found in Equation 5.1, giving a lower bound to the solution. Moreover, it is important to ensure that the solution meets all the constraints imposed in the problem, for instance, if a point from which backward and forward propagation is conducted is defined, continuity needs to be assured. In addition, the trajectory should be able to go from the initial and to the final orbit. To make sure that this happens with the maneuvers found, an external software could be used. In this case, this software is going to be FreeFlyer.

It is important to note that this project will include external functions that have already been programmed, both by DLR colleagues and by external sources. These functions will only be used in this project after a validation of the solutions is performed in order to ensure that they are not going to become sources of error.

9.1 Freeflyer

FreeFlyer is a commercial off-the-shelf software from AI Solutions used for space mission design, analysis, and operations. It provides the scripting language needed to solve many types of astrodynamics problems. It is used by many agencies including DLR and NASA, as it has been verified and validated. (AISolutions, 2022).

Freeflyer will be used for verification of the results, as an initial visualization, and as a primary way of trying and testing ideas, as it is user-friendly and very helpful. Nevertheless, the final software that is going to be developed throughout the thesis will be completely independent from it, as one of the main requirements of DLR is to have an autonomous software not dependent on commercial software.

Chapter 10

Conclusions and Thesis Structure

10.1 Main conclusions

After the study performed during this literature study, many interesting conclusions have been reached concerning the initial proposed questions, which where:

- *What types Earth-Moon transfers are possible? Which ones are the most useful for the current and near-future lunar missions?*
- *Which optimization possibility can achieve the best solution from an engineering perspective? What is the best way to model this optimization? What are the main objectives that should be studied?*

Concerning the first question, many possible transfers have been found, nevertheless, it was decided that the most interesting one for the project that is going to be conducted during the master thesis is a direct transfer, due to their short transfer time, their opportunities for optimization, the possibility of calculating them both using an inertial reference frame and a model like the CR3BP, and because they have been greatly used in lunar missions both in the past and in the present. In addition, it was decided that the initial orbit is going to be taken as an Earth-bounded orbit, and the final state is going to be taken as a Moon-bounded orbit, and hence other transfers did not offer as much benefits. Moreover, due to the increasing interest on the possibilities that a WSB offers to reduce the ΔV, a study of the possibility of including these transfers in the same software will also be conducted.

Concerning the second question, it was found that both gradient-based algorithms and genetic algorithms offer different ways of solving optimization problems. A large amount of research has been done using evolutionary algorithms for lunar transfers, as they can deal with complex, non-continuous functions and do not need a good initial guess. On the other hand, gradient-based algorithms offer a quicker way of finding the most optimal solution if a good initial guess is given, as they make use of the previous knowledge of the problem. Therefore, it was decided that some research would be conducted on the actual viability of using these optimizers for direct transfers. In addition, it was also found that hybrid algorithms offer a good balance between both, using the genetic algorithm to find the best initial guess for the gradient-based algorithm, which will then be used for refinement. This method will also be studied. Concerning the dynamical model, the final aim of this project is to obtain a result that copes with the defined objectives including the full dynamical model. To do so, several steps will be followed, including an initial optimization with a simpler model, for instance the CR3BP, whose solution can become the initial guess for a model which includes additional perturbations.

Moreoever, it was decided that, due to its characteristics and availability in the DLR functions, a variable-order variable-step size Adams-Bashforth-Moulton is going to used as the integrator in addition to a Cowell propagator. Concerning the objectives, it was decided that a single-objective optimization is going to be performed, nevertheless, it is of great interest to study the best way of modelling these objectives so that the user can decide depending on its needs.

10.2 Research questions

After all the main conclusions have been stated, the main research questions for the master thesis will be defined as:

What are the most optimal Earth-Moon direct transfers, considering a user-defined objective, from a user-defined Earth-bounded orbit to a user-defined Moon-bounded orbit including a full dynamical model?

From this main question, several subquestions would be included in order to precisely establish the main objectives of this research. To deal with the fact that it has to be possible for the user to define its mission objectives and initial and final orbits, the following two questions will need to be answered.

What is the best way to define objectives so that they can be modified by the user?

How can initial and final orbits be modelled so that any could be used for the optimization?

Secondly, as an optimized solution including a full dynamical model can not be found directly, a good initial guess will need to be obtained. Hence becoming very important to answer the following question.

How can an accurate initial guess for a further optimization be obtained?

To study the different optimizers in order to come up with the best solution in a reasonable amount of time, the next question will need to be answered.

Is it possible to use a gradient-based optimizer to optimize direct transfers to the Moon? If a genetic algorithm is needed to obtain a good initial guess, is a gradient-based optimizer useful for the solution refinement?

Lastly, due to the great scientific interest, and as a lower priority task if enough time is available, two additional subquestions will be included. *Can manifold transfers be included even if a full dynamical model is used in an inertial frame if the initial guess is calculated using the CR3BP formulation?*

Is it reasonable to include Weak Stability Boundary transfers as a possible solution for the optimizations of direct transfers incorporating an additional constraint?

The main task of the future master thesis is to generate a software able to optimize lunar transfers. This software should be flexible and general so that it can be used for different missions.

10.3 Thesis Structure

This master thesis project will be divided in three parts. Firstly, to obtain the initial guess for the gradient-based optimization with the full model in Fortran (11 weeks). This will be done in a gradual way, using simple models with easy solutions, using a genetic algorithm to optimize the transfer with a simpler model, and/or using some ready-to-use tools that are open source and that offer many possibilities, such as SEMPY. Secondly, to conduct the gradient-based optimization using the full dynamical model in python (7 weeks). Then, to evaluate the results obtained, validate them and verify them (4 weeks). Lastly, the master thesis report needs to be finished (2 weeks).

Table 10.1: Master thesis schedule

Task	**Duration**	**Dates**
Initial guess generation	11 weeks	
Familiarization with SEMPY package in Python	1 week	9-13 Jan
Study all the possibilities in the CR3BP package	1 week	16-20 Jan
Definition of initial and final Keplerian orbits in the CR3BP	3 days	23-25 Jan
Demonstrate Lambert transfer	3 days	26-30 Jan
Define the optimization objective, constraints and design variables	1 week	31-7 Feb
Set optimization parameters	1 week	8-15 Feb
Optimization using the genetic algorithm	3 weeks	16-9 March
Extract solutions from CR3BP to ECI to use as the initial guess	1 week	10-16 March
Write report	1 week	17-23 March
Software development	7 weeks	
Verify and validate the DLR Fortran functions	3 days	24-28 March
Generate the propagator of the transfer with the full dynamical model	2 weeks	29-12 Apr
Set optimization parameters	1 week	13-20 Apr
Write report	1 week	14-20 Apr
Run, evaluate, validate and verify the results	4 weeks	
Run optimizer and obtain results	2 weeks	21-5 May
Evaluate and analyze the results	2 weeks	8-19 May
Compare against results in other papers	1 week	22-25 May
Use results with FreeFlyer	1 week	29-2 June
Write report	3 days	5-8 June
Finish the report	2 weeks	9-23 June

Bibliography

AISolutions (2022). *FreeFlyer Features Overview*. URL: https://ai-solutions.com/_help_Files/freeflyer_features_overview.htm (visited on 09/27/2022).

Alessi, Elisa, Gerard Gómez, and Josep Masdemont (2010). "Two-manoeuvres transfers between LEOs and Lissajous orbits in the Earth–Moon system". In: *Advances in Space Research* 45.10, pp. 1276–1291. ISSN: 0273-1177. DOI: 10.1016/j.asr.2009.12.010.

Almeida Junior, Allan Kardec de and Antonio Fernando Bertachini de Almeida Prado (2022). "Comparisons between the circular restricted three-body and bi-circular four body problems for transfers between the two smaller primaries". In: *Scientific Reports* 12.1, pp. 1–19.

Ariane 5 User's Manual (2008). URL: http://www.arianespace.%20com/launch-services-ariane5/Ariane-5-User%E2%80%99s-Manual.asp (visited on 11/15/2022).

Belbruno, E (2000). "Low Energy Trajectories for Space Travel Using Stability Transition Regions". In: *IFAC Proceedings Volumes* 33.2. IFAC Workshop on Lagrangian and Hamiltonian Methods for Nonlinear Control, Princeton, NJ, USA, 16-18 March 2000, pp. 7–12. ISSN: 1474-6670. DOI: 10.1016/S1474-6670(17)35540-4.

– (1987). "Lunar capture orbits, a method of constructing earth moon trajectories and the lunar GAS mission". In: *19th International Electric Propulsion Conference*, p. 1054.

Belbruno, E and J Carrico (2000). "Calculation of weak stability boundary ballistic lunar transfer trajectories". In: *Astrodynamics Specialist Conference*, p. 4142.

Belbruno, E, M Gidea, and F Topputo (2010). "Weak stability boundary and invariant manifolds". In: *SIAM Journal on Applied Dynamical Systems* 9.3, pp. 1061–1089.

Belbruno, E and J Miller (1990). "A ballistic lunar capture trajectory for the Japanese spacecraft hiten". In: *Jet Propulsion Laboratory, IOM* 312, pp. 90–4.

– (Feb. 1991). "Method for the construction of a lunar transfer trajectory using ballistic capture". In: 75.

– (1993). "Sun-perturbed Earth-to-Moon transfers with ballistic capture". In: *Journal of Guidance, Control, and Dynamics* 16.4, pp. 770–775.

Berry, R (1970). "Launch window and translunar, lunar orbit, and trans-earth trajectory planning and control for the Apollo 11 lunar landing mission". In: *8th Aerospace Sciences Meeting*, p. 24.

Biesbroek, Robin and Guy Janin (2000). "Ways to the Moon". In: *ESA bulletin* 103, pp. 92–99.

BlueOrigin (2022). *Blue origin - Back to the Moon to stay*. URL: https://www.blueorigin.com/blue-moon/ (visited on 11/26/2022).

Britannica (2022a). *Basic planetary data - Earth*. URL: https://www.britannica.com/place/Earth/Basic-planetary-data (visited on 11/30/2022).

– (2022b). *Moon*. URL: https://www.britannica.com/place/Moon (visited on 11/30/2022).

– (2022c). *Newton's law of gravitation*. URL: https://www.britannica.com/science/Newtons-law-of-gravitation (visited on 12/12/2022).

Cacolici, Gianna Nicole et al. (2017). "Stability of Lagrange Points: James Webb Space Telescope". In: *The University of Arizona*.

Cakaj, Shkelzen, Werner Keim, and Krešimir Malarić (2007). "Communications duration with low earth orbiting satellites". In: *The Forth IASTED International Conference on Antennas, Radar and Wave Propagation*.

Canalias, E and J Masdemont (Oct. 2007). "Homoclinic and heteroclinic transfer trajectories between Lyapunov orbits in the Sun-Earth and Earth-Moon systems". In: *IEEC Departament de Matemàtica Aplicada I, Universitat Politècnica de Catalunya*.

Cellier, François E. and Ernesto Kofman (2006). "Multi-step Integration Methods". In: *Continuous System Simulation*. Boston, MA: Springer US, pp. 117–164. ISBN: 978-0-387-30260-7. DOI: 10.1007/0-387-30260-3_4.

Ceriotti, Matteo, Camilla Colombo, and Massimiliano Vasile (Jan. 2006). "Trajectory design and optimisation for lunar transfer". In: *1st Hellenic-European Student Space Science and Technology Symposium*.

Chapman, Allan (Feb. 2009). "A new perceived reality: Thomas Harriot's Moon maps". In: *Astronomy and Geophysics* 50.1, pp. 1.27–1.33. ISSN: 1366-8781. DOI: 10.1111/j.1468-4004.2009.50127.x.

Chobotov, Vladimir A (2002). *Orbital mechanics*. 3rd. Reston, VA: AIAA Education Series.

Chong, Edwin KP and Stanislaw H Zak (2013). *An introduction to optimization*. Vol. 75. John Wiley & Sons.

Circi, Christian and Paolo Teofilatto (2006). "Weak stability boundary trajectories for the deployment of lunar spacecraft constellations". In: *Celestial Mechanics and Dynamical Astronomy* 95.1, pp. 371–390.

Cowan, Kevin (2021a). "Interplanetary trajectories - gravity-assist maneuvers". In: *Delft University of Technology*. [Power Point slides].

– (2021b). "Three-body problem". In: *Delft University of Technology*. [Power Point slides].

De La Torre, D, R Flores, and Elena Fantino (2018). "On the solution of Lambert's problem by regularization". In: *Acta Astronautica* 153, pp. 26–38.

Faller, J. E., . Kenneth L. Nordtvedt, and . Alan H Cook (2022). *Gravity, Encyclopedia Britannica*. URL: https://www.britannica.com/science/gravity-physics (visited on 12/12/2022).

Farquhar, Robert W. (1971). "The Utilization of Halo Orbits in Advanced Lunar Operations". In: National Aeronautics and Space Administration.

Fernandes, Sandro and Cleverson Marinho (Jan. 2012). "Sun influence on two-impulsive Earth-to-Moon transfers". In: *Journal of Aerospace Engineering, Sciences and Applications* 4, pp. 82–91. DOI: 10.7446/jaesa.0401.08.

Folta, David and David Quinn (2006). "Lunar Frozen Orbits". In: *AIAA/AAS Astrodynamics Specialist Conference and Exhibit*. DOI: 10.2514/6.2006-6749.

Gargioni, Gustavo et al. (Mar. 2019). "Multiple Asteroid Retrieval Mission from Lunar Orbital Platform-Gateway Using Reusable Spacecrafts". In: pp. 1–13. DOI: 10.1109/AERO.2019.8741985.

Goldberg, D (1989). *Genetic Algorithms in Search, Optimization, and Machine Learning*. AddisonWesley.

Gomez, G et al. (Jan. 2000). "Dynamics and mission design near libration points. Vol. 1: Fundamentals: The case of collinear libration points". In: *World Scientific Monograph Series in Mathematics*.

Gómez, G. and J.M. Mondelo (2001). "The dynamics around the collinear equilibrium points of the RTBP". In: *Physica D: Nonlinear Phenomena* 157.4, pp. 283–321. ISSN: 0167-2789. DOI: 10.1016/S0167-2789(01)00312-8.

Goswami, JN and M Annadurai (2009). "Chandrayaan-1: India's first planetary science mission to the Moon". In: *Current science*, pp. 486–491.

Hohenkerk, C.Y. et al. (1992). "Celestial reference systems". In: *Explanatory Supplement to the Astronomical Almanac*, pp. 111–114.

Hohmann, Walter (1925). "Die Erreichbarkeit der Himmelskörper". In: *Die Erreichbarkeit der Himmelskörper*. Oldenbourg Wissenschaftsverlag.

Horn, MK and KH Well (1983). "Numerical solution of piecewise continuous trajectory optimization problems". In: *IFAC Proceedings Volumes* 16.8, pp. 81–89.

Hosseini, S (Jan. 2011). "An Exploration Of Fuel Optimal Two-impulse Transfers To Cyclers in the Earth-Moon System". MA thesis. University of California, Irvine.

Howell, K. C., D. L. Mains, and B. T. Barden (1994). "Transfer trajectories from Earth parking orbits to Sun-Earth halo orbits". In: *Spaceflight mechanics 1994*, pp. 399–422.

Huckfeldt, Moritz (2020). "Study of Space-Environmental Effects on Interplanetary Trajectories". MA thesis. University of Bremen. URL: https://elib.dlr.de/142099/.

Jung, Seungyun and Youdan Kim (2017). "Formation Flying Along Halo Orbit Using Switching Hamiltonian Structure-Preserving Control". In: *7th European Conference for Aeronautics and Aerospace Science*, pp. 2017–39.

Kara, Ozan and Çağrı Kılıç (2015). "Comprehensive study of small satellite Moon missions: Architecture design, electric propulsion system optimization and cost analysis". In: DOI: 10.13140/RG.2.1.2770.2487.

Kemble, Stephen (Jan. 2006). *Interplanetary Mission Analysis and Design*. Berlin: Springer. ISBN: 3-540-29913-0.

Können, GP and J Meeus (1972). "Extreme declinations of the moon." In: *Journal of the British Astronomical Association* 82, pp. 192–193.

Koon, Wang Sang et al. (2001). "Low energy transfer to the Moon". In: *Celestial Mechanics and Dynamical Astronomy* 81.1, pp. 63–73.

Lange, TJ de et al. (2008). "Conceptual Design of a Streamlined Mission to Compete for the Google Lunar X PRIZE". In: *To Moon and Beyond*. Deutsche Geselschaft fur Luft-und Raumfahrt, pp. 1–10.

Lara, Martín, Bernard De Saedeleer, and Sebastián Ferrer (2009). "Preliminary design of low lunar orbits". In: *Proceedings of the 21st International Symposium on Space Flight Dynamics*.

Liu, Yuxin, Ron Noomen, and Pieter Visser (2021). "A gravity assist mapping for the circular restricted three-body problem using Gaussian processes". In: *Advances in Space Research* 68.6, pp. 2488–2500.

Lo, Martin W et al. (2001). "Genesis mission design". In: *The Journal of the astronautical sciences* 49.1, pp. 169–184.

McCarthy, Brian P. (Jan. 2019). "Characterization of Quasi-Periodic Orbits for Applications in the Sun-Earth and Earth-Moon Systems". In: DOI: 10.25394/PGS.7423658.v1.

Mengali, Giovanni and Alessandro A Quarta (2005). "Optimization of biimpulsive trajectories in the earth-moon restricted three-body system". In: *Journal of Guidance, Control, and Dynamics* 28.2, pp. 209–216.

Merritt, P (1996). "Continuous communications for the lunar farside: How do we get there? A differentially corrected halo transfer orbit". In: *34th Aerospace Sciences Meeting and Exhibit*.

Michael, W and R Tolson (1960). *Effect of eccentricity of the lunar orbit, oblateness of the earth, and solar gravitational field on lunar trajectories*. National Aeronautics and Space Administration.

Miele, A and S Mancuso (2000). "Optimal trajectories for earth–moon–earth flight". In: *Acta Astronautica* 49.2, pp. 59–71.

Mooij, Erwin and Dominic Dirkx (2022). "Propagation and Optimisation in Astrodynamics - Global Optimisation". In: *Delft University of Technology*. [Power Point slides].

Moulton, F.R (1920). *Periodic Orbits*. Vol. 2. (in collaboration with D.Buchanan, T.Buck, F.Griffin, W.Longley, and W.MacMillan). Washington D.C: Carnegie Institute of Washington.

Nakamiya, Masaki et al. (Jan. 2007). "Analysis of capture trajectories to libration points". In: *Advances in the Astronautical Sciences* 127.

Newton, Isaac (1723). *Philosophiae naturalis principia mathematica. Auctore Isaaco Newtono,..* sumptibus Societatis.

– (1687). "Principia mathematica". In: *Book III, Lemma V, Case* 1, p. 1687.

Ockels, J. W. and Robin Biesbroek (1999). "Genetic algorithms used to determine WSB trajectories for the lunarsat mission". In: *Artificial Intelligence, Robotics and Automation in Space*. Vol. 440.

Parker, Jeffrey (2018). "ASEN 5050 - Spaceflight dynamics - Solar Radiation Pressure". In: *University of Colorado - Boulder*. [Power Point slides].

Parker, Jeffrey (Jan. 2006). "Families of low-energy lunar Halo transfers". In: *Advances in the Astronautical Sciences* 124.

Parker, Jeffrey and R. Anderson (2013). *Low-Energy Lunar Trajectory Design*. Vol. 12. DESCANSO, JPL Deep-Space Communications and Navigation Series. Jet Propulsion Laboratory, California Institute of Technology.

Pederzoli, Luciano (Nov. 2011). *The megalith builders - Psychic archaeology and the Nuragic civilization*.

Perozzi, Ettore and Alessio Di Salvo (2008). "Novel spaceways for reaching the Moon: an assessment for exploration". In: *Celestial Mechanics and Dynamical Astronomy* 102.1, pp. 207–218.

PIKAIA (2022). URL: `http://www.hao.ucar.edu/modeling/pikaia/pikaia.php` (visited on 11/29/2022).

Poincaré, Henri (1967). *New methods of celestial mechanics*. Vol. 2. National Aeronautics and Space Administration.

Quantius, Dominik et al. (June 2012). "Weak stability boundary transfer to the Moon from GTO as a piggyback payload on Ariane 5". In: *CEAS Space Journal* 3. DOI: `10.1007/s12567-012-0024-3`.

Rast, Rina et al. (2017). "Effects of the Moon on the Earth in the Past, Present and Future". In: *USURJ: University of Saskatchewan Undergraduate Research Journal* 4.1.

Rosengren, Aaron J. et al. (Apr. 2015). "Chaos in navigation satellite orbits caused by the perturbed motion of the Moon". In: *Monthly Notices of the Royal Astronomical Society* 449.4, pp. 3522–3526. ISSN: 0035-8711. DOI: `10.1093/mnras/stv534`. eprint: `https://academic.oup.com/mnras/article-pdf/449/4/3522/18507434/stv534.pdf`. URL: `https://doi.org/10.1093/mnras/stv534`.

Roy, AE and MW Ovenden (1955). "On the occurrence of commensurable mean motions in the solar system: the mirror theorem". In: *Monthly Notices of the Royal Astronomical Society* 115.3, pp. 296–309.

Russell, C and V Angelopoulos (2011). "The ARTEMIS mission". In: *The ARTEMIS mission*. Springer, pp. 3–25.

Seefelder, W (2000). "Transfer Trajectories for the Lunarsat Mission". In: *Exploration and Utilisation of the Moon*. Vol. 462, p. 245.

Shampine, L. F. and M. K. Gordon (May 1976). "Computer Solution of Ordinary Differential Equations: The Initial Value Problem". In: *The Computer Journal* 19.2, pp. 155–155. ISSN: 0010-4620. DOI: `10.1093/comjnl/19.2.155`.

Sidorenko, Vladislav (2014). "Distant retrograde orbits for the Moon's exploration". In: *40th COSPAR Scientific Assembly* 40, B0–1.

Smith, C et al. (1989). "Mean and apparent place computations in the new IAU system. I-The transformation of astrometric catalog systems to the equinox J2000. 0." In: *The Astronomical Journal* 97, pp. 265–279.

Smith, Marshall et al. (2020). "The Artemis Program: An Overview of NASA's Activities to Return Humans to the Moon". In: *2020 IEEE Aerospace Conference*, pp. 1–10. DOI: `10.1109/AERO47225.2020.9172323`.

Spurmann, J. (Feb. 2010). *Lunar Transfer Trajectories*. Tech. rep. TN 10-02. Germany: GSOC - DLR.

Tantardini, Marco et al. (Nov. 2010). "Spacecraft trajectories to the L3 point of the Sun–Earth three-body problem". In: *Celestial Mechanics and Dynamical Astronomy* 108, pp. 215–232. DOI: `10.1007/s10569-010-9299-x`.

Tatay, Jose (2019). "Optimal Trajectories in the Earth-Moon CR3BP system." MA thesis. TU Delft.

Topputo, Francesco, Massimiliano Vasile, and FRANCO BERNELLI-ZAZZERA (2005). "Earth-to-Moon Low Energy Transfers Targeting L1 Hyperbolic Transit Orbits". In: *Annals of the New York Academy of Sciences* 1065.1, pp. 55–76.

Uesugi, K (1996). "Results of the MUSES-A "HITEN" mission". In: *Advances in Space Research* 18.11, pp. 69–72.

USNavalObservatory (2010). *The Astronomical Almanac for the year 2010*. Washington, DC: US Government Printing Office.

Vikhar, Pradnya A. (2016). "Evolutionary algorithms: A critical review and its future prospects". In: *2016 International Conference on Global Trends in Signal Processing, Information Computing and Communication (ICGTSPICC)*, pp. 261–265. DOI: 10.1109/ICGTSPICC.2016.7955308.

Villac, BF and DJ Scheeres (2003). "New class of optimal plane change maneuvers". In: *Journal of guidance, control, and dynamics* 26.5, pp. 750–757.

Watts, H. A. and L. F. Shampine (1986). "Smoother Interpolants for Adams Codes". In: *SIAM Journal on Scientific and Statistical Computing* 7.1, pp. 334–345. DOI: 10.1137/0907022.

Weber, Bryan (2022). *The Jacobi Constant*. URL: https://ai-solutions.com/_help_Files/freeflyer_features_overview.htm (visited on 12/08/2022).

Wikipedia (2022). *Lunar precession*. URL: https://en.wikipedia.org/wiki/Lunar_precession (visited on 12/12/2022).

WolframResearch (2007). *Modified Julian Date*. URL: https://scienceworld.wolfram.com/astronomy/ModifiedJulianDate.html (visited on 08/16/2022).

Yazdi, Kian and Ernst Messerschmid (2004). "Analysis of parking orbits and transfer trajectories for mission design of cis-lunar space stations". In: *Acta Astronautica* 55.3. New Opportunities for Space. Selected Proceedings of the 54th International Astronautical Federation Congress, pp. 759–771. ISSN: 0094-5765. DOI: 10.1016/j.actaastro.2004.05.006.

Young, Dr. Judith S. (2022). *Moon teachings for the masses at the UMASS Sunwheel and around the world: The major lunar standstills of 2006 and 202-2025*. URL: https://www.umass.edu/sunwheel/pages/moonteaching.html (visited on 11/10/2022).

Zazzera, Franco Bernelli, Francesco Topputo, and Mauro Massari (2004). "Assessment of mission design including utilization of libration points and weak stability boundaries". In: *ESA Advanced Concept Team*.

Zimovan, Emily M, Kathleen C Howell, and Diane C Davis (2017). "Near rectilinear halo orbits and their application in cis-lunar space". In: *3rd IAA Conference on Dynamics and Control of Space Systems, Moscow, Russia*. Vol. 20, p. 40.